



# Quarkonium production measurement in Pb-Pb collisions with the ALICE experiment at the LHC

**Lizardo Valencia Palomo**

**Institut de Physique Nucléaire d'Orsay  
(CNRS-IN2P3, Université Paris-Sud 11)**

**for the ALICE collaboration**

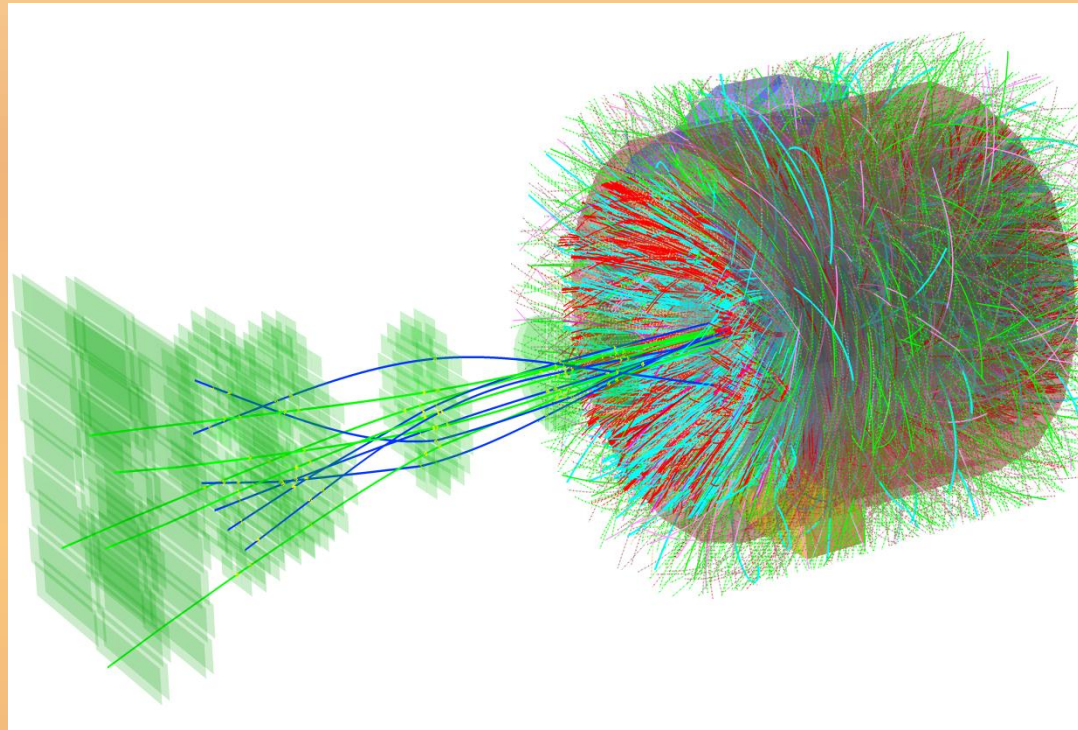
*5th International Workshop on Heavy  
Quark Production in Heavy-ion Collisions*

Utrecht University, Netherlands

November 14-17, 2012

# Outline

- Physics motivations.
- The ALICE experiment.
- Analysis:
  - ❑  $J/\psi \rightarrow ee$  ( $|y| < 0.9$ ).
  - ❑  $J/\psi \rightarrow \mu\mu$  ( $2.5 < y < 4.0$ ).
- Results:
  - ❑  $J/\psi$   $R_{AA}$  vs  $N_{part}$ ,  $y$  and  $p_T$ .
  - ❑  $J/\psi$   $\langle p_T \rangle$ .
- $\psi(2S) \rightarrow \mu\mu$ .
- Conclusions.

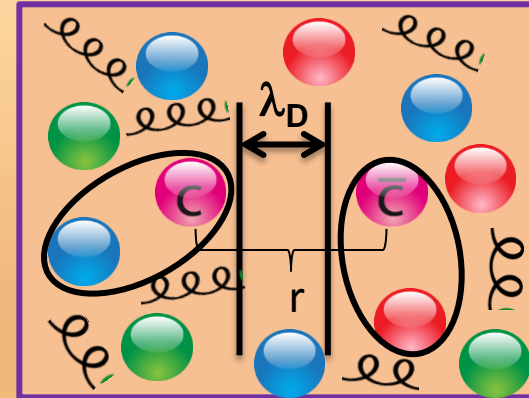


# Quarkonium in A-A

- Ultrarelativistic heavy-ion collisions  $\rightarrow$  high energy densities.
- Quark Gluon Plasma: deconfined state of quarks and gluons.

Quarkonium as a probe of deconfinement:

- ✓ Created in the early stages of the collision.
- ✓ Suppressed by Debye screening.
- ✓ Different radii & bounding energies  $\rightarrow$  sequential suppression.

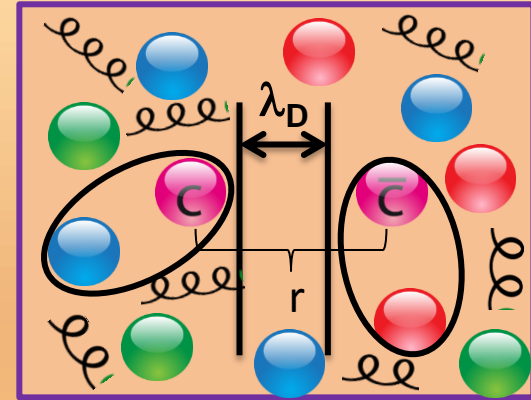


# Quarkonium in A-A

- Ultrarelativistic heavy-ion collisions  $\rightarrow$  high energy densities.
- Quark Gluon Plasma: deconfined state of quarks and gluons.

Quarkonium as a probe of deconfinement:

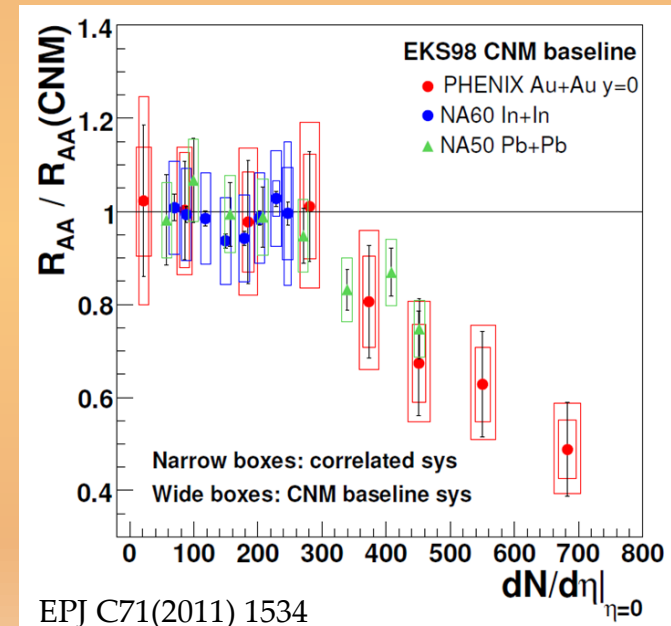
- ✓ Created in the early stages of the collision.
- ✓ Suppressed by Debye screening.
- ✓ Different radii & bounding energies  $\rightarrow$  sequential suppression.



Quarkonium production in A-A previously studied by different experiments:

- ❑ Significant  $J/\psi$  suppression beyond the Cold Nuclear Matter effects.
- ❑ Suppression is practically  $\sqrt{s}$  - independent.
- ❑ Is quarkonium regeneration playing a role?

$$R_{AA} = \frac{Y_{A-A}^{J/\psi}}{\langle N_{Coll} \rangle Y_{pp}^{J/\psi}}$$

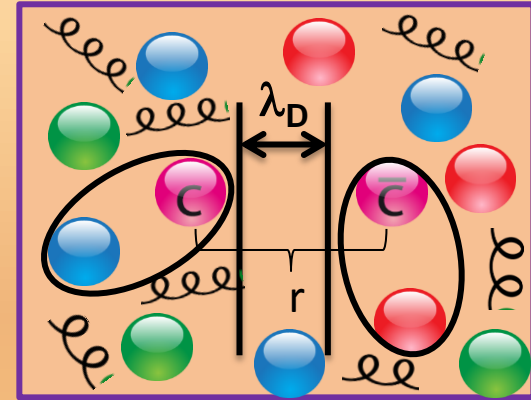


# Quarkonium in A-A

- Ultrarelativistic heavy-ion collisions  $\rightarrow$  high energy densities.
- Quark Gluon Plasma: deconfined state of quarks and gluons.

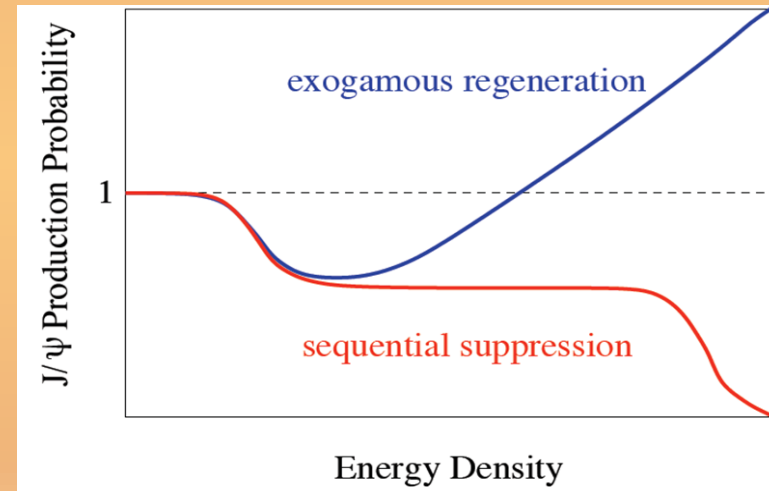
Quarkonium as a probe of deconfinement:

- ✓ Created in the early stages of the collision.
- ✓ Suppressed by Debye screening.
- ✓ Different radii & bounding energies  $\rightarrow$  sequential suppression.



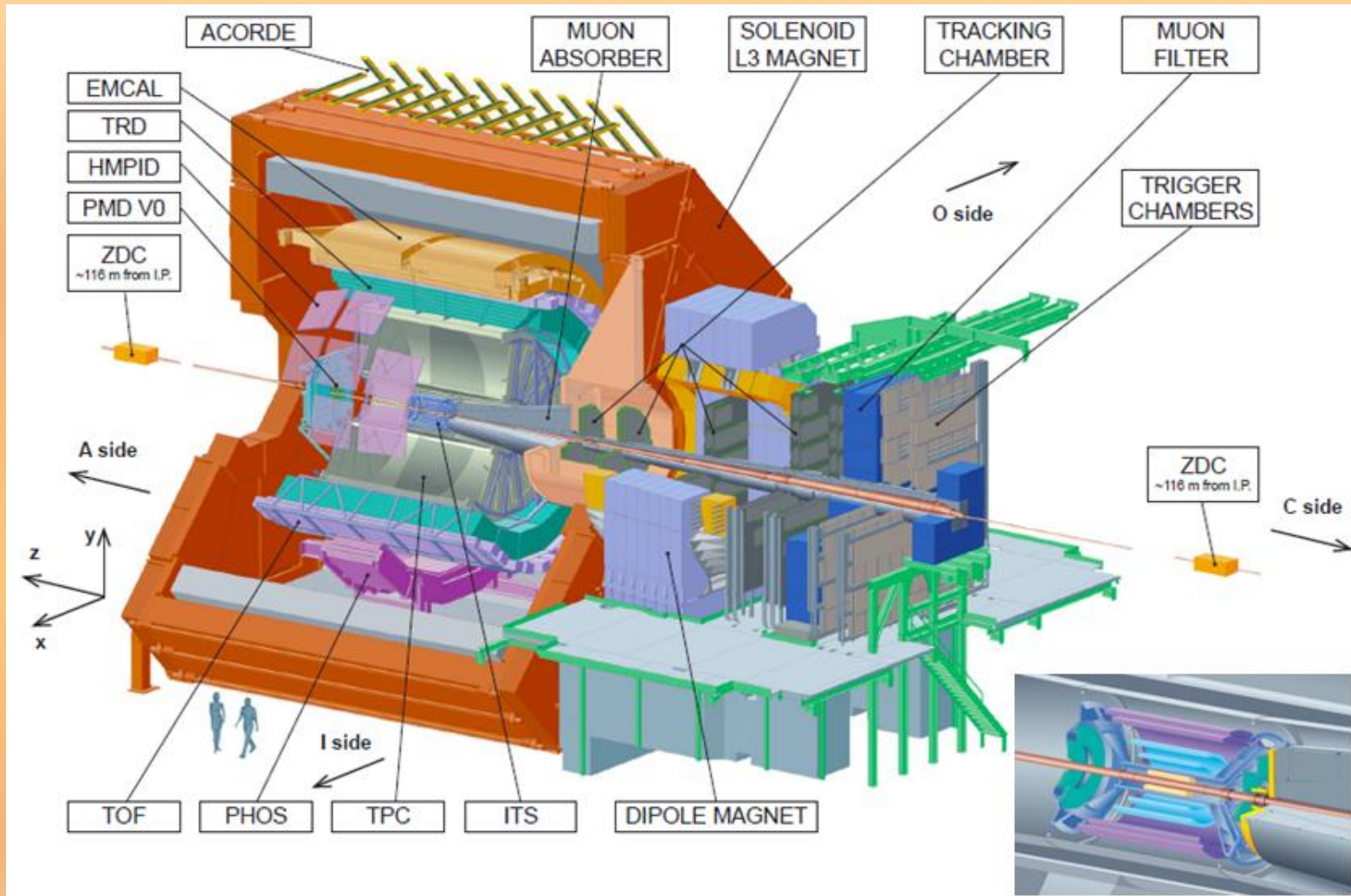
What can we expect at the LHC?

1. New collision energy regime  
 $\rightarrow$  **larger suppression?**
2.  $N_{c\bar{c}}$ /central collision  $\approx 10 \times$  RHIC  
 $\rightarrow$  **measurable effects from regeneration?**

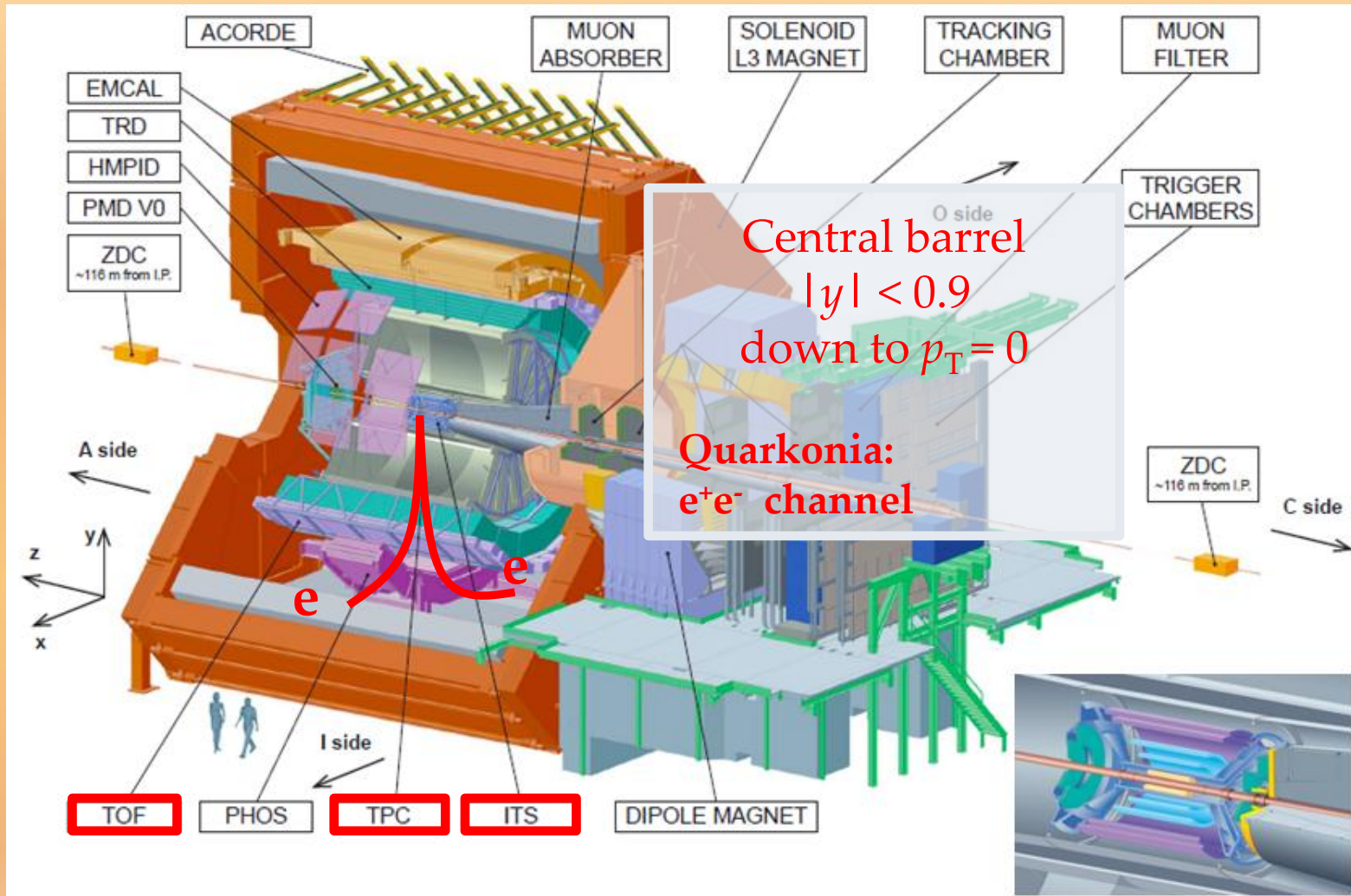




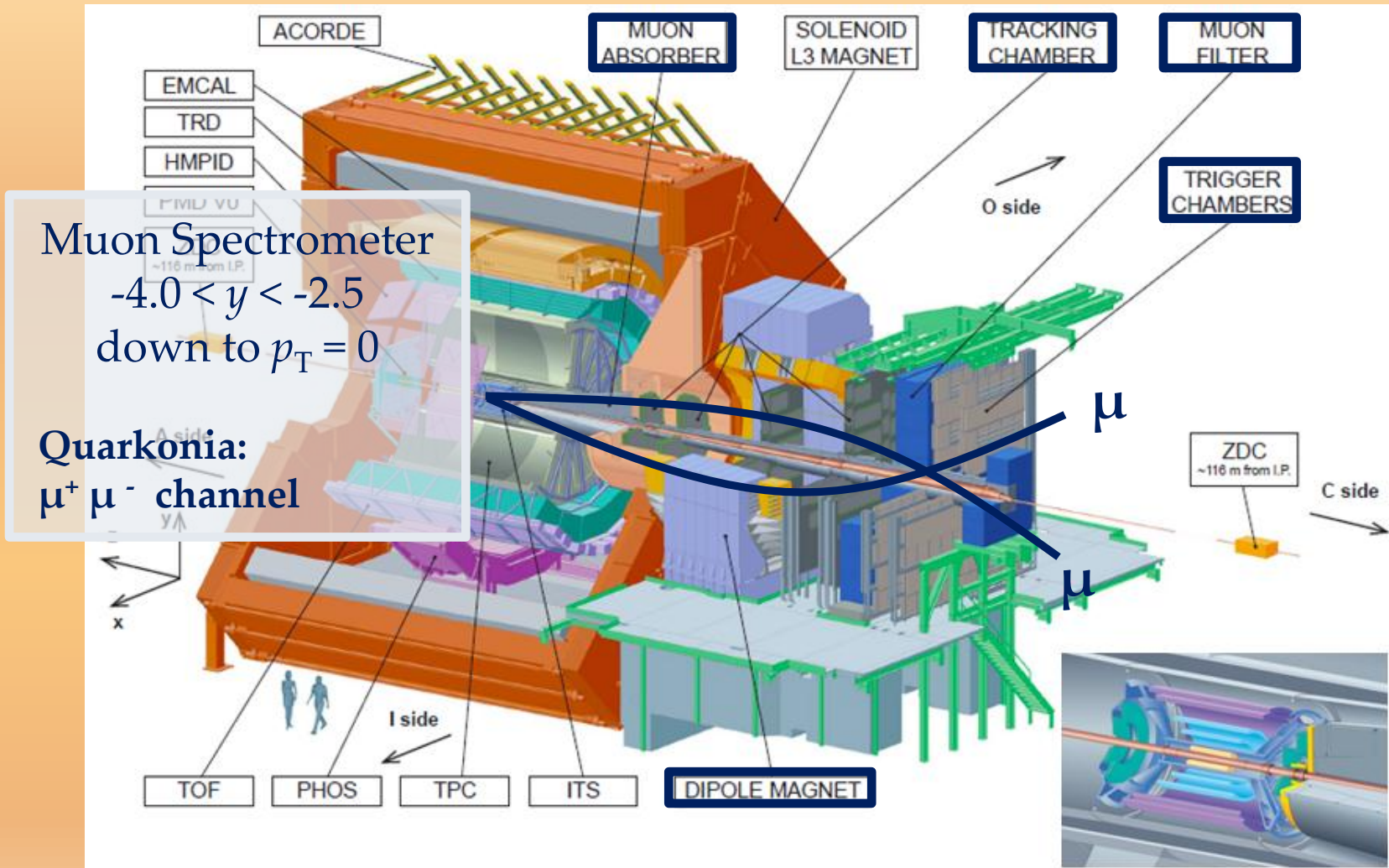
# The ALICE experiment



# The ALICE experiment



# The ALICE experiment





# Trigger, event selection and centrality

➤  $J/\psi \rightarrow ee$ :

2010 + 2011 data set: Minimum Bias (MB) and centrality triggered events  $\rightarrow L_{\text{int}} \approx 15 \mu\text{b}^{-1}$ .

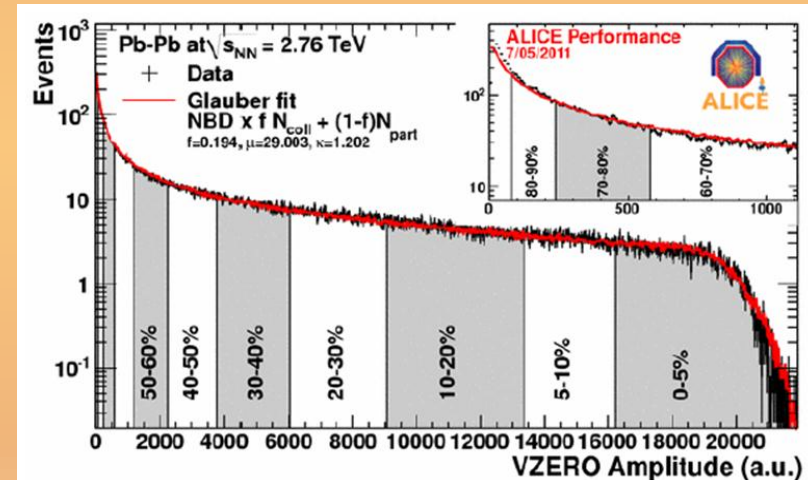
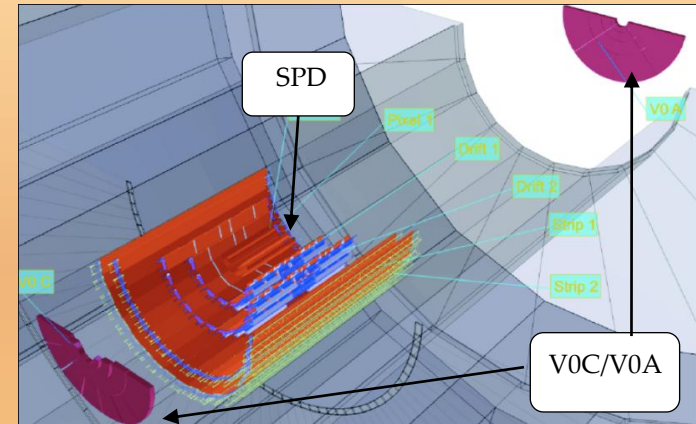
2010 MB trigger: signal in two hodoscope scintillators (V0A and V0C) and in the outer layer of a pixel detector (SPD)  $\rightarrow L_{\text{int}} \approx 2 \mu\text{b}^{-1}$ .

2011 Centrality triggered events  $\rightarrow L_{\text{int}} \approx 15 \mu\text{b}^{-1}$ .

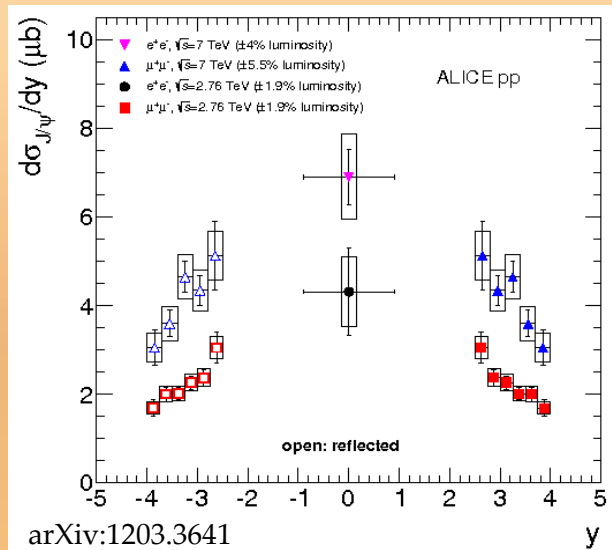
➤  $J/\psi, \psi(2S) \rightarrow \mu\mu$ :

2011 data set: dimuon events from the muon trigger,  $L_{\text{int}} \approx 70 \mu\text{b}^{-1}$ .

Centrality estimation is based on a Glauber model fit of the V0 amplitude.



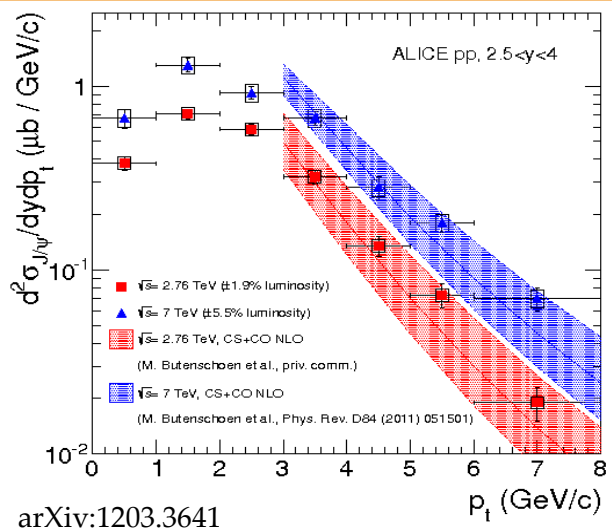
# pp measurement at $\sqrt{s} = 2.76$ TeV



Reference from pp collisions is needed!

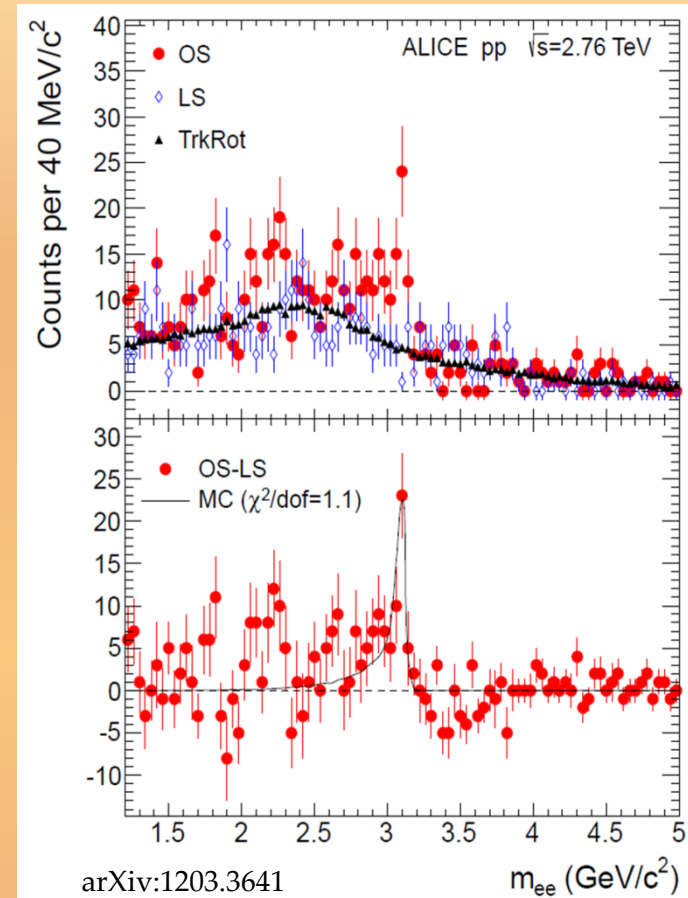
Both at forward and midrapidity.

$2.5 < y < 4.0$ : NRQCD calculations describe the measured  $d^2\sigma/dydp_T$  at 7 and 2.76 TeV.

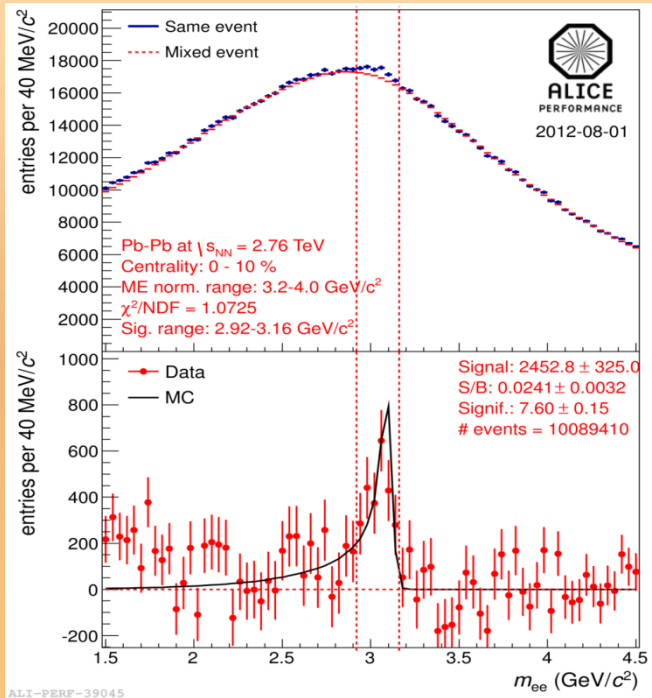


pp reference is the main source of systematics in the  $R_{AA}$ :

- 9% for  $J/\psi \rightarrow \mu\mu$ .
- 26% for  $J/\psi \rightarrow ee$ .

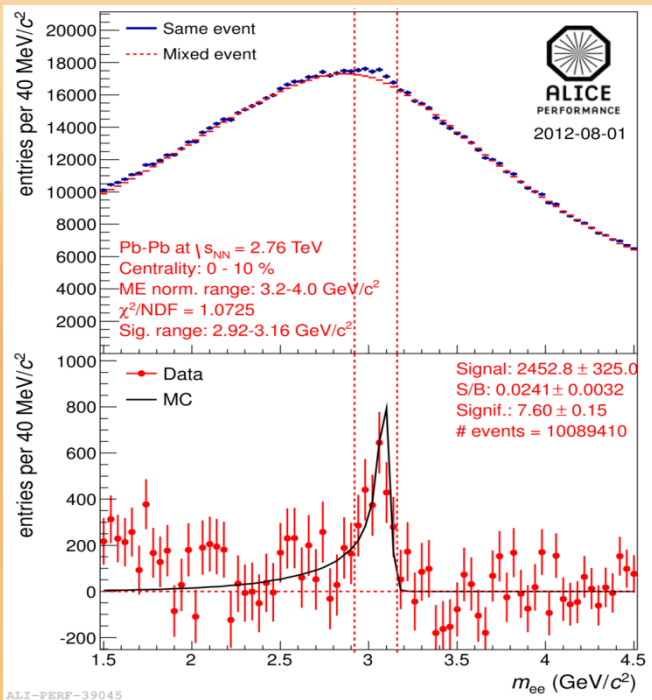


# J/ψ → ee in Pb-Pb: Analysis

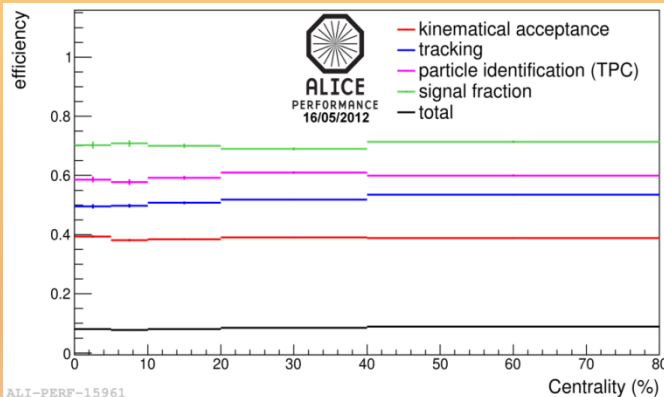


- ✓ J/ψ yield obtained by subtracting the background from the opposite sign dielectron invariant mass spectrum using the mixed event technique.
- ✓ The MC signal includes the bremsstrahlung of the electrons in the detector material.
- ✓ Signal extracted in three centrality bins: 0-10%, 10-40% and 40-80%.

# J/ψ → ee in Pb-Pb: Analysis



- ✓ J/ψ yield obtained by subtracting the background from the opposite sign dielectron invariant mass spectrum using the mixed event technique.
- ✓ The MC signal includes the bremsstrahlung of the electrons in the detector material.
- ✓ Signal extracted in three centrality bins: 0-10%, 10-40% and 40-80%.



- ✓ Efficiency computed using HIJING enriched with J/ψ.
- ✓ Little dependence on the centrality.



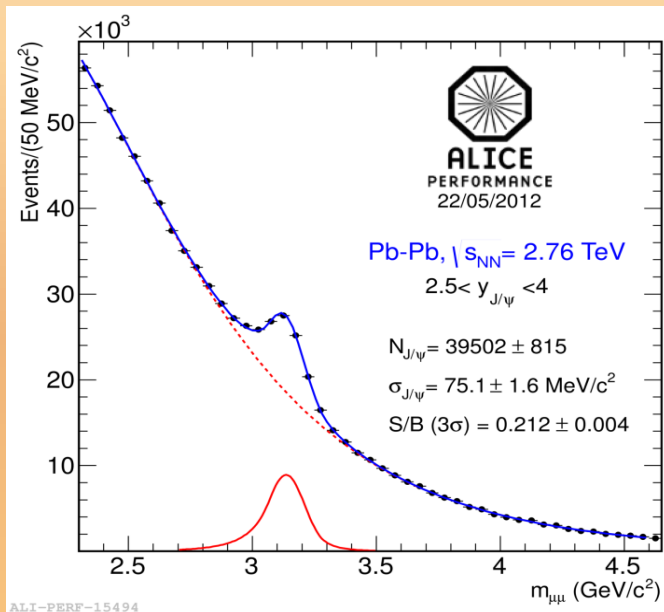
# $J/\psi \rightarrow \mu\mu$ in Pb-Pb: analysis

2011 statistics allows the extraction of  $J/\psi$  yields in narrow  $y$ ,  $p_T$  and centrality bins.

Yield extracted by fitting the unlike sign invariant dimuon mass spectrum:

- ✓ Signal: modified Crystal Ball.
- ✓ Background: different functions. Also subtracted using the event mixing technique.

Results are then combined to obtain a mean weighted  $N_{J/\psi}$  and to extract systematic uncertainties on signal extraction.



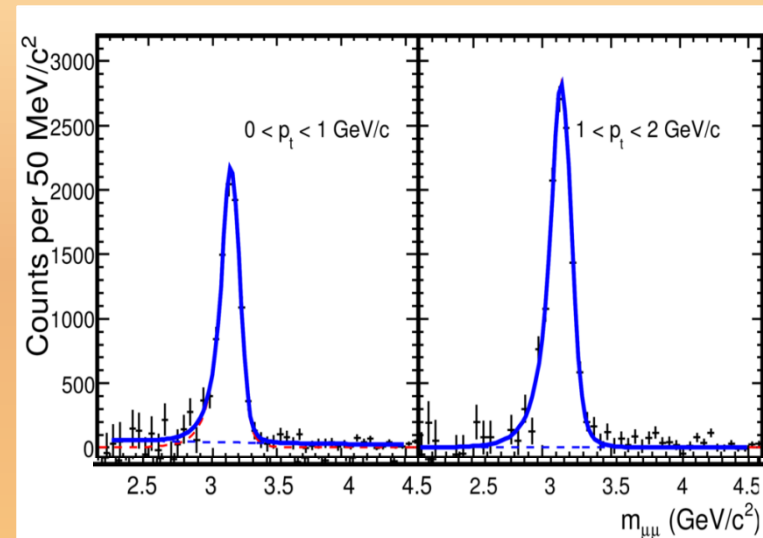
# $J/\psi \rightarrow \mu\mu$ in Pb-Pb: analysis

2011 statistics allows the extraction of  $J/\psi$  yields in narrow  $y$ ,  $p_T$  and centrality bins.

Yield extracted by fitting the unlike sign invariant dimuon mass spectrum:

- ✓ Signal: modified Crystal Ball.
- ✓ Background: different functions. Also subtracted using the event mixing technique.

Results are then combined to obtain a mean weighted  $N_{J/\psi}$  and to extract systematic uncertainties on signal extraction.



# $J/\psi \rightarrow \mu\mu$ in Pb-Pb: analysis

2011 statistics allows the extraction of  $J/\psi$  yields in narrow  $y$ ,  $p_T$  and centrality bins.

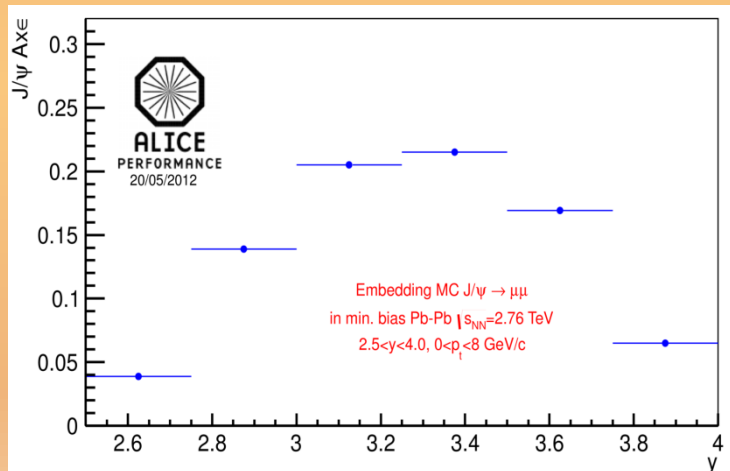
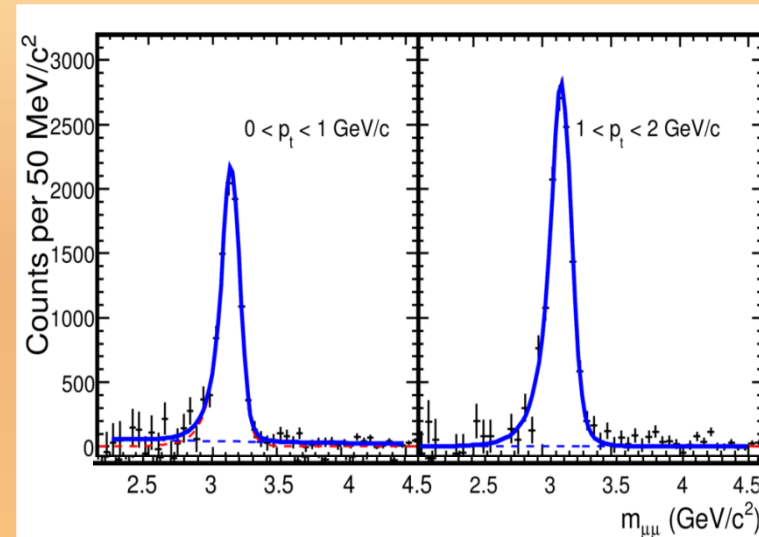
Yield extracted by fitting the unlike sign invariant dimuon mass spectrum:

- ✓ Signal: extended Crystal Ball.
- ✓ Background: different functions. Also subtracted using the event mixing technique.

Results are then combined to obtain a mean weighted  $N_{J/\psi}$  and to extract systematic uncertainties on signal extraction.

Acceptance  $\times$  efficiency values are obtained by embedding MC  $J/\psi$  into real events.

Rapidity bins: detector acceptance.



# J/ψ → μμ in Pb-Pb: analysis

2011 statistics allows the extraction of J/ψ yields in narrow  $y$ ,  $p_T$  and centrality bins.

Yield extracted by fitting the unlike sign invariant dimuon mass spectrum:

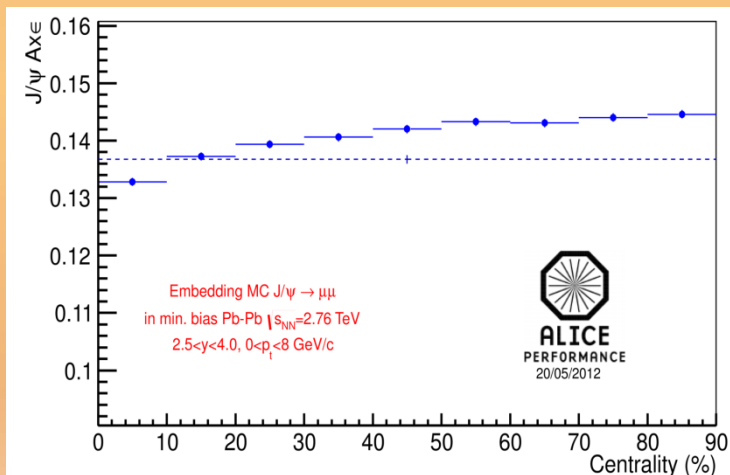
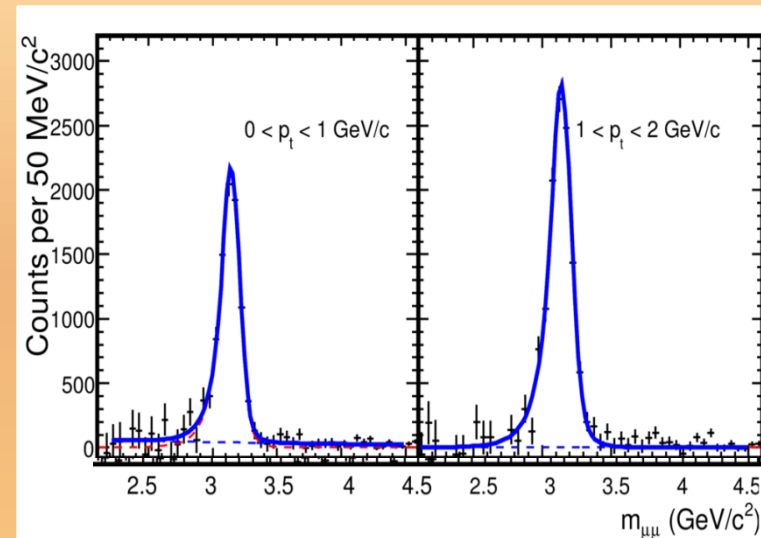
- ✓ Signal: extended Crystal Ball.
- ✓ Background: different functions. Also subtracted using the event mixing technique.

Results are then combined to obtain a mean weighted  $N_{J/\psi}$  and to extract systematic uncertainties on signal extraction.

Acceptance x efficiency values are obtained by embedding MC J/ψ into real events.

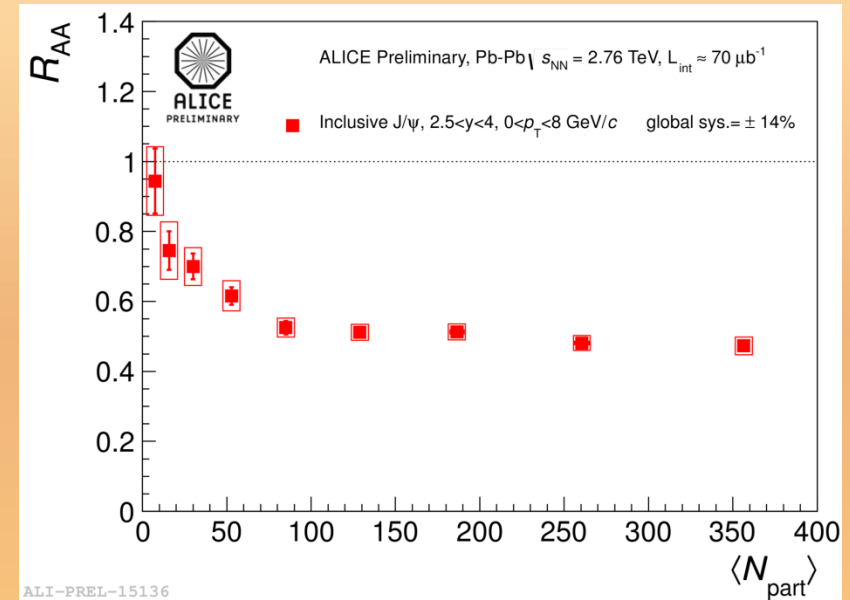
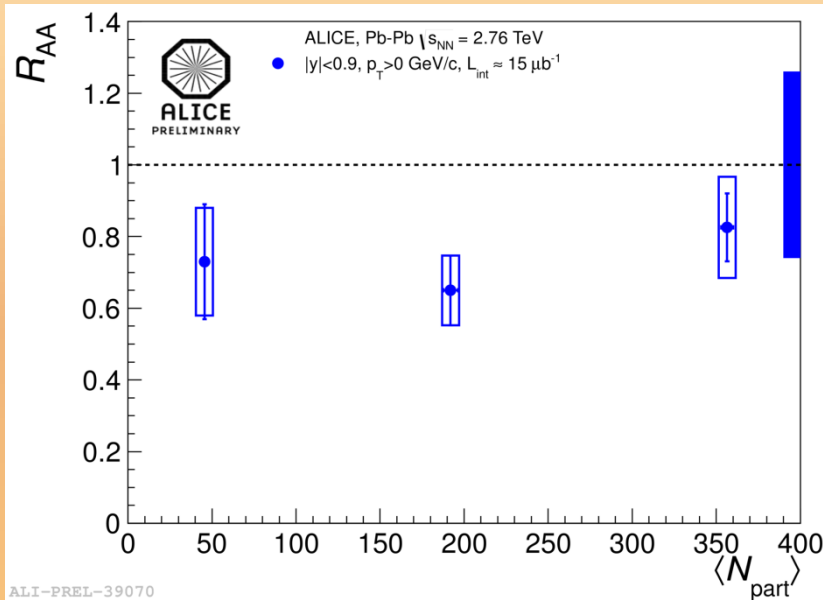
Rapidity bins: detector acceptance.

Weak centrality dependence.



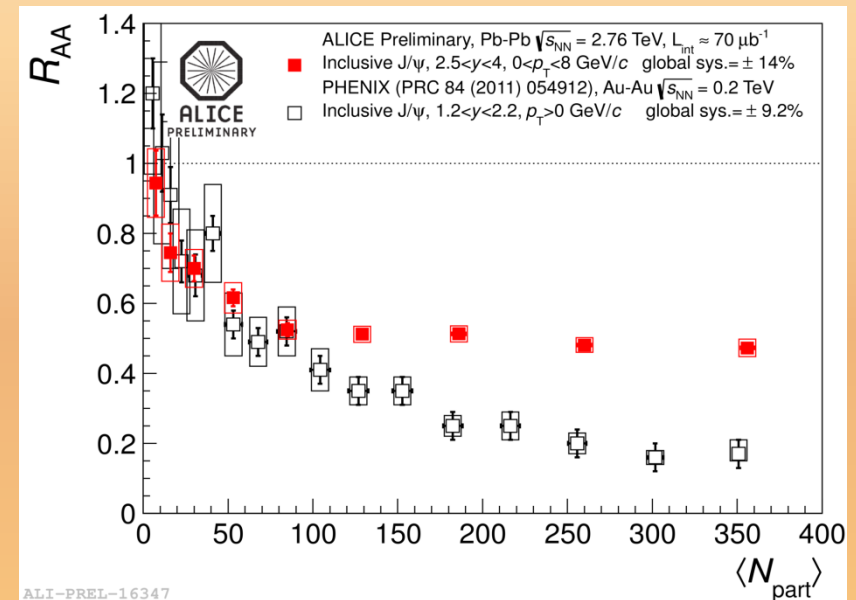
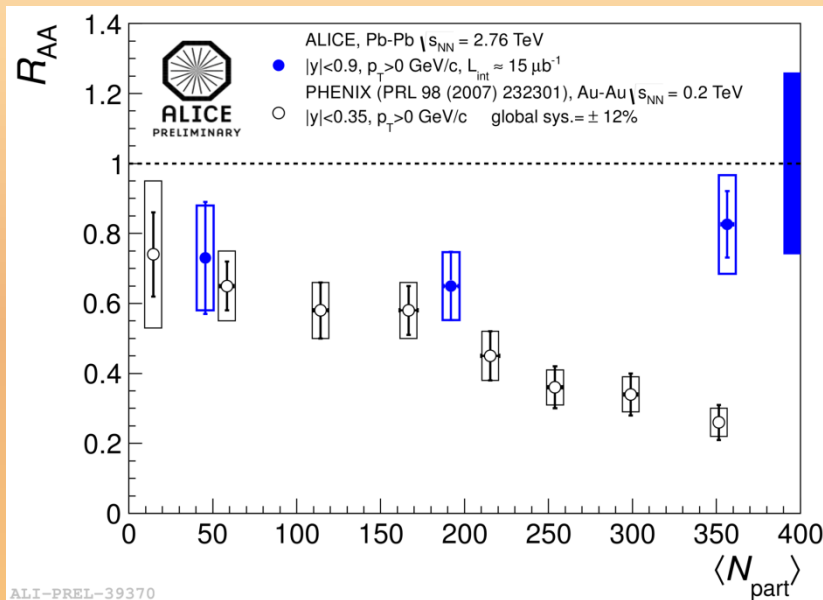


# Results: $J/\psi$ $R_{AA}$ vs centrality



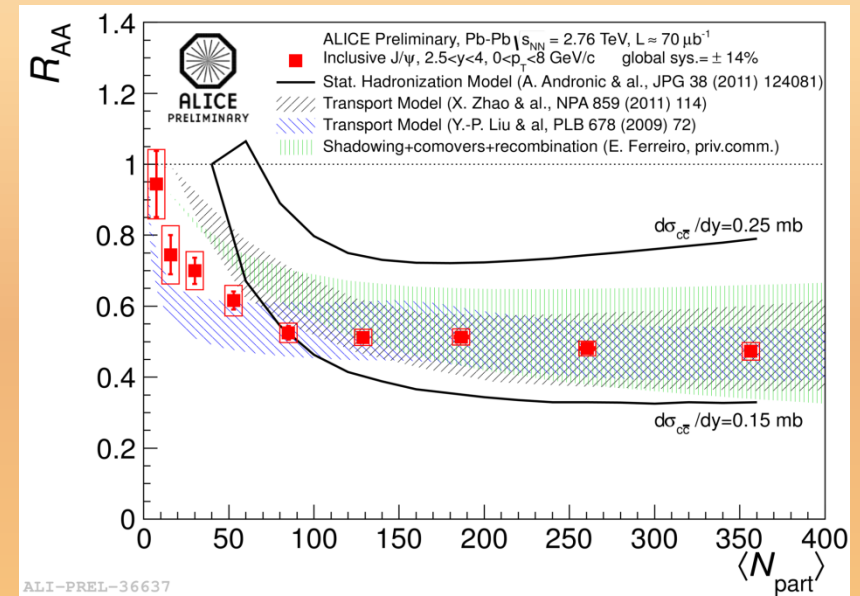
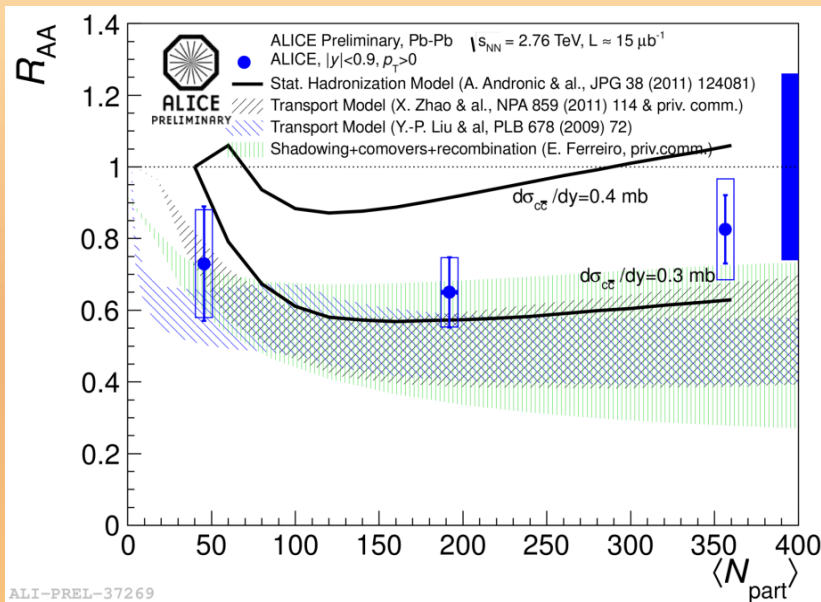
- No significant centrality dependence within errors.
- No significant centrality dependence for  $N_{part} > 100$ .

# Results: $J/\psi$ $R_{AA}$ vs centrality



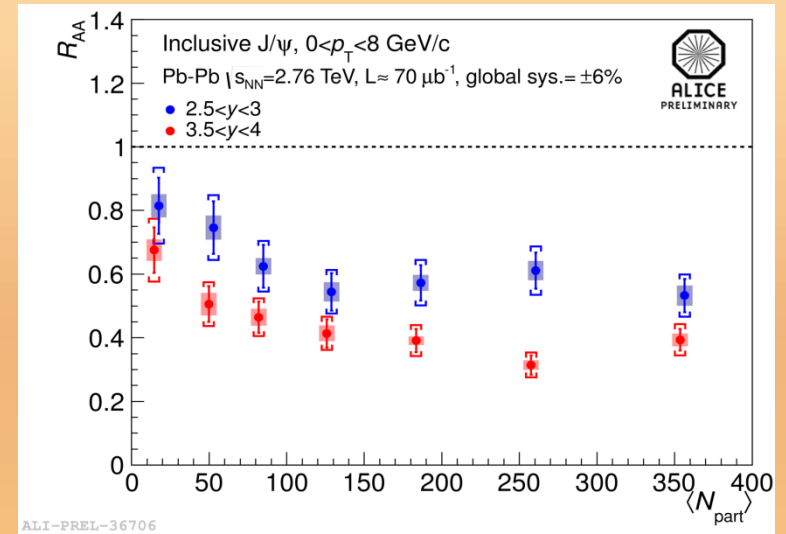
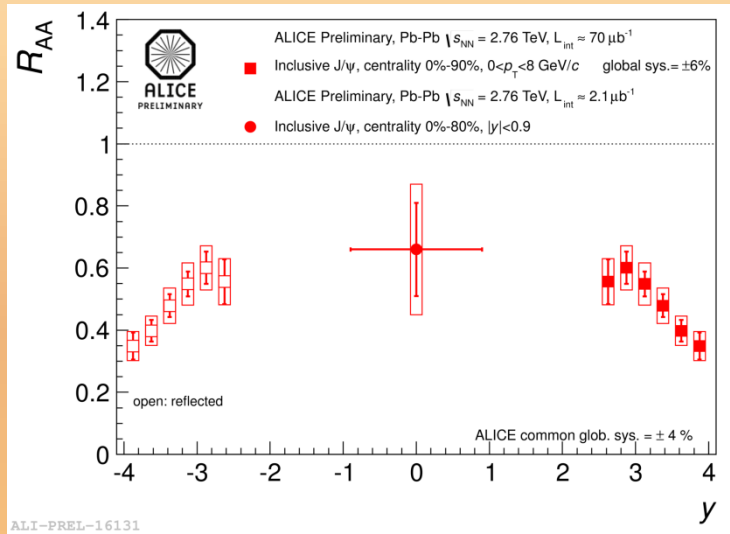
- No significant centrality dependence within errors.
- No significant centrality dependence for  $N_{part} > 100$ .
- $R_{AA}$  in the most central collision from ALICE is  $\sim 3$  times larger than at PHENIX.
- $R_{AA}^{ALICE} \sim 3 \times R_{AA}^{PHENIX}$  for  $N_{part} > 200$ .

# Results: $J/\psi$ $R_{AA}$ vs centrality



- Statistical Hadronisation Model: prediction for two  $d\sigma_{c\bar{c}}/dy$ .
- Transport Models: different rate equations of  $J/\psi$  dissociation and regeneration in QGP, in both cases more than 50% of measured yield in the most central collisions due to  $J/\psi$  regeneration, the rest is from initial production.
- Green band: includes shadowing, comovers and recombination.
- Need to measure Cold Nuclear Matter effects.

# Results: $J/\psi$ $R_{AA}$ vs centrality, $y$ bins

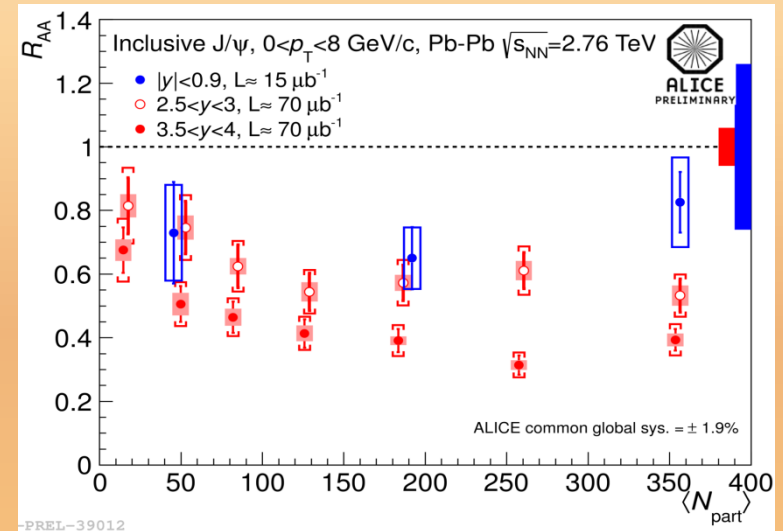
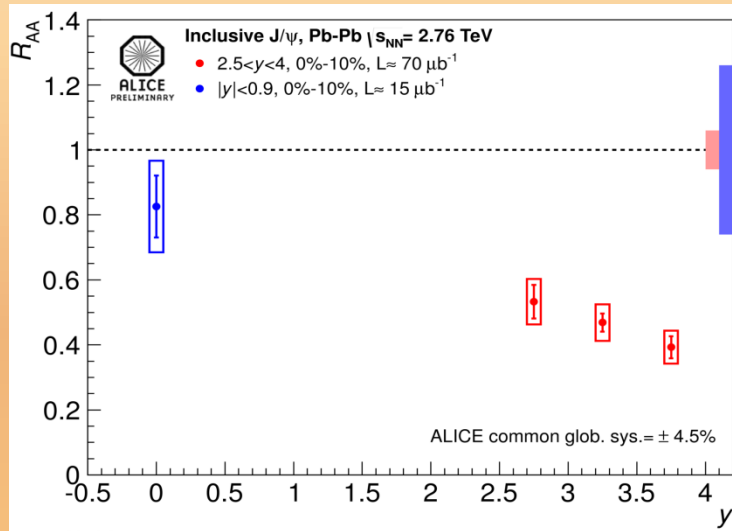


$R_{AA}$  decreases by 40% from  $y = 2.5$  to  $y = 4$ .

Same centrality behavior at forward  $y$ .



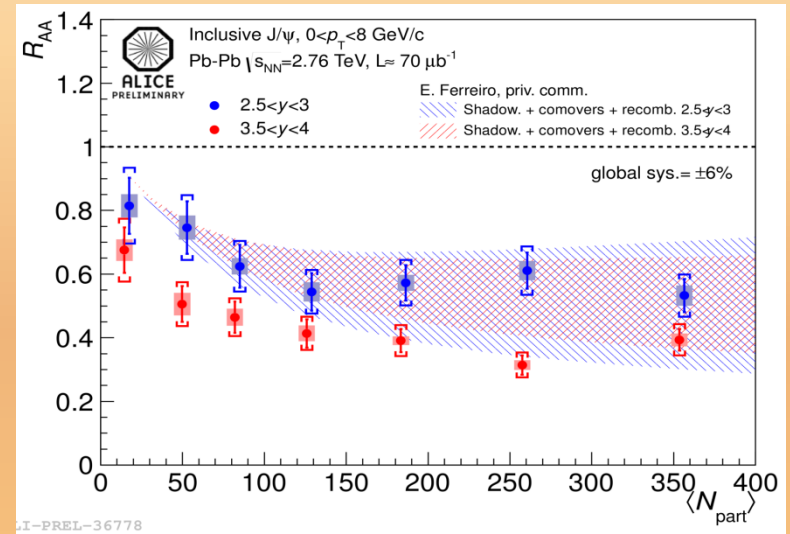
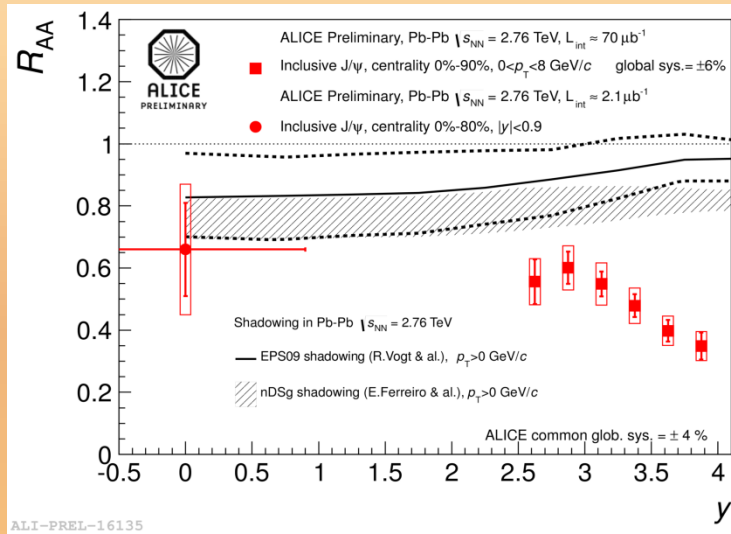
# Results: $J/\psi$ $R_{AA}$ vs centrality, $y$ bins



$R_{AA}$  decreases by 40% from  $y = 2.5$  to  $y = 4$ . Same centrality behavior at forward  $y$ .

Hint of smaller suppression at mid rapidity than at forward rapidity in the most central collisions.

# Results: $J/\psi$ $R_{AA}$ vs centrality, $y$ bins



$R_{AA}$  decreases by 40% from  $y = 2.5$  to  $y = 4$ .

Same centrality behavior at forward  $y$ .

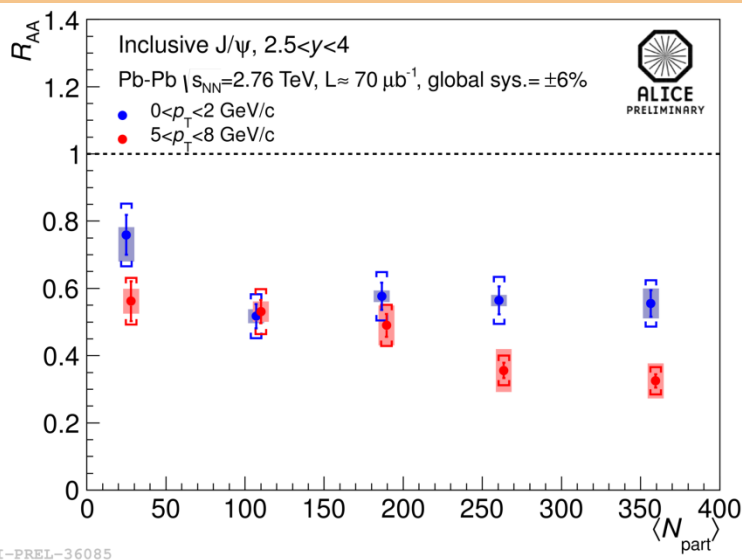
Hint of smaller suppression at mid rapidity than at forward rapidity in the most central collisions.

$J/\psi$  less suppressed if shadowing calculations are considered.

Weaker  $y$  dependence predicted by shadow. + comovers + recombination.

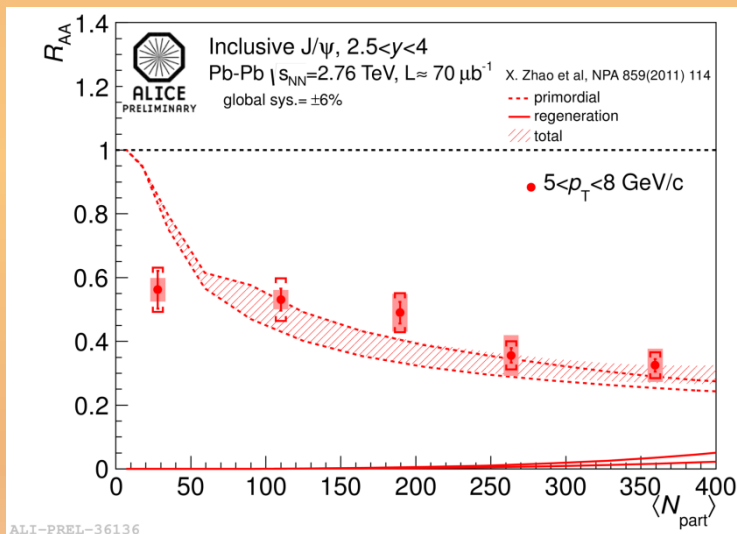
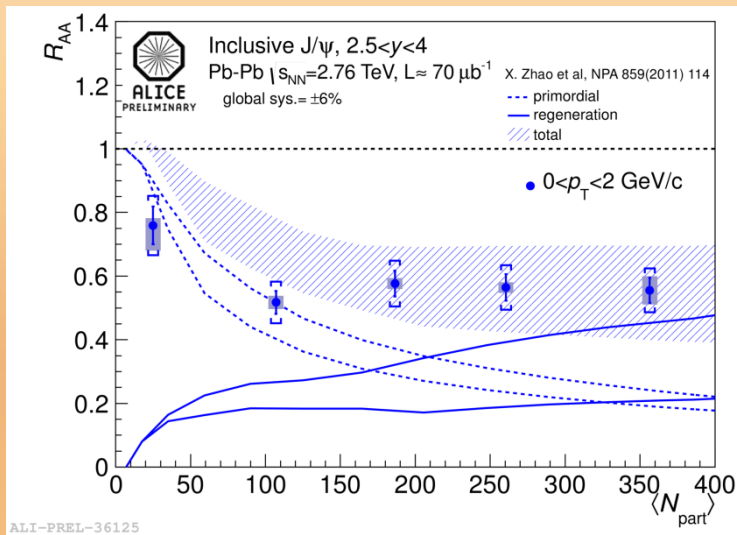
Cold Nuclear Matter effects need to be quantified!

# Results: $J/\psi$ $R_{AA}$ vs centrality, $p_T$ bins



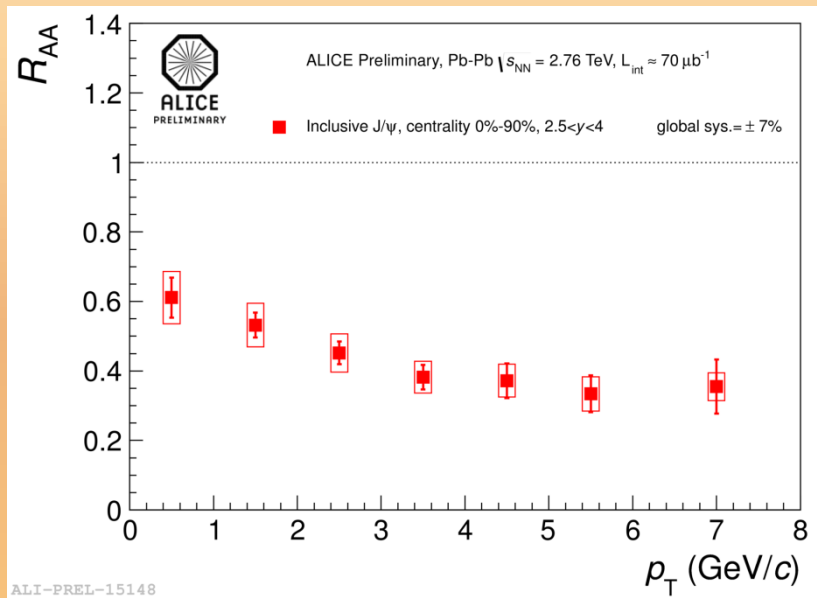
- Stronger suppression for high- $p_T$   $J/\psi$ .
- No centrality dependence for low- $p_T$   $J/\psi$  when  $N_{\text{part}} > 100$ .

# Results: $J/\psi$ $R_{AA}$ vs centrality, $p_T$ bins

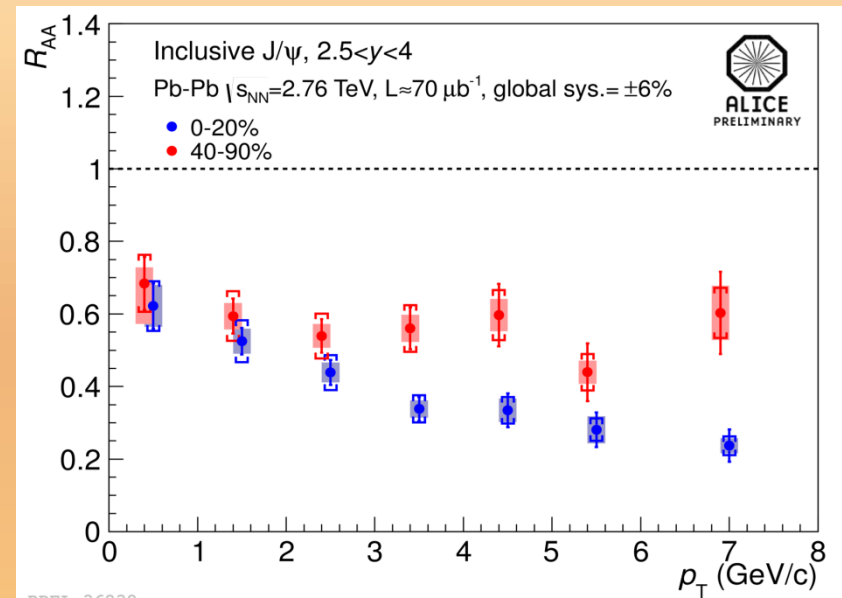


- Stronger suppression for high- $p_T$   $J/\psi$ .
- No centrality dependence for low- $p_T$   $J/\psi$  when  $N_{\text{part}} > 100$ .
- Consistent behavior with (re)combination.
- Good agreement between data and Transport Model.
- Around 50% of the low- $p_T$   $J/\psi$  are produced by (re)combination.
- For high- $p_T$   $J/\psi$  this contribution is very small.

# Results: $J/\psi$ $R_{AA}$ vs $p_T$ , centrality bins

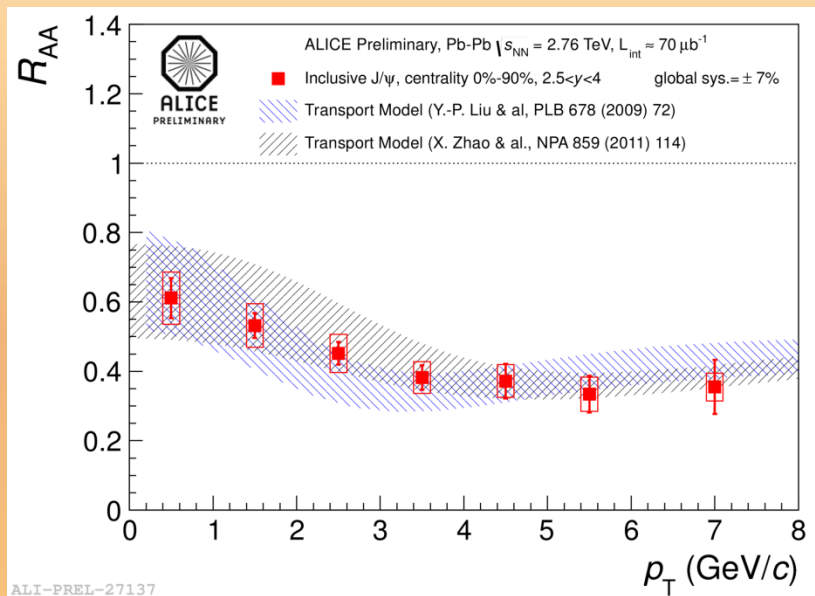


Stronger suppression for high- $p_T$   $J/\psi$ .



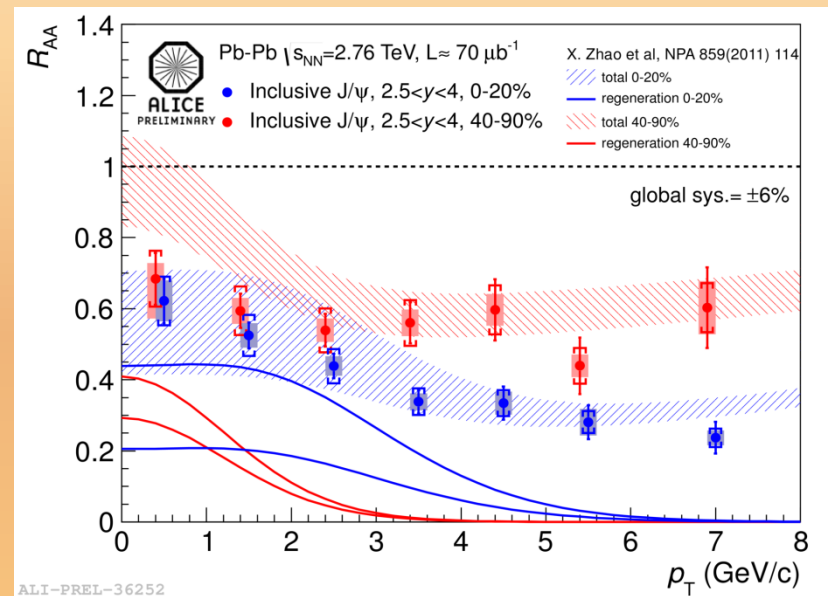
Stronger  $p_T$  dependence for central collisions.

# Results: $J/\psi$ $R_{AA}$ vs $p_T$ , centrality bins



Stronger suppression for high- $p_T$   $J/\psi$ .

Very good agreement with Transport Models.



Stronger  $p_T$  dependence for central collisions.

Discrepancy between model and data at low- $p_T$  in peripheral collisions.

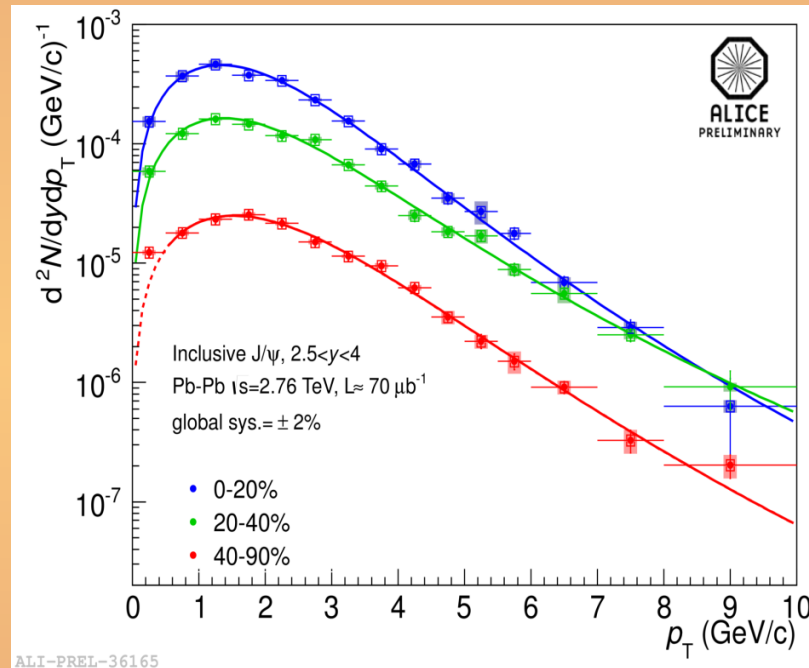
Regeneration at work in the low- $p_T$  regime.



# Results: $J/\psi < p_T >$

$< p_T >$  values were obtained by fitting  $\frac{d^2 N}{dy dp_T} \propto \frac{p_T}{[1 + (p_T / p_0)^2]^n}$  in three

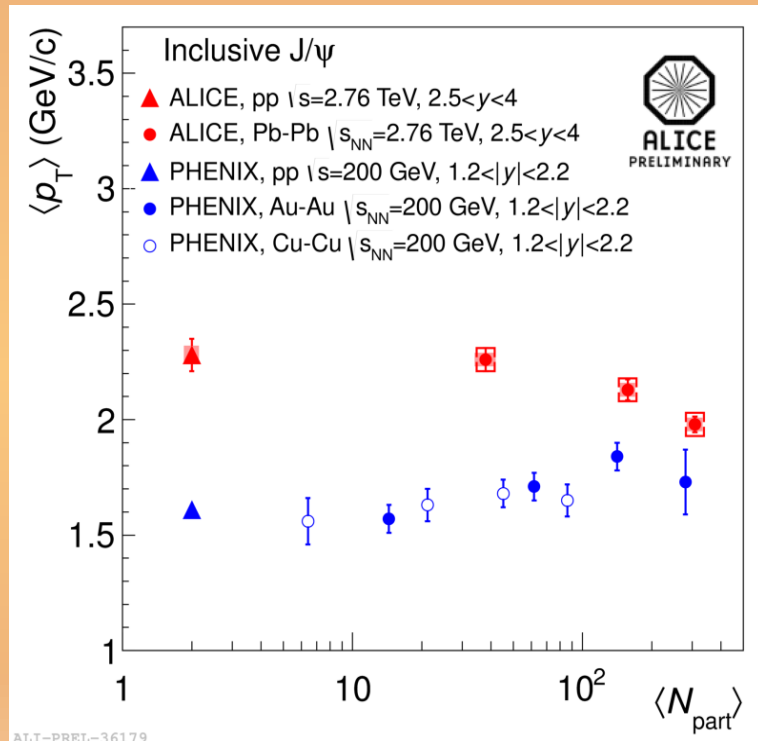
different centrality bins. Low- $p_T$  excess in the most peripheral bin due to non-hadronic production.



# Results: $J/\psi < p_T >$

$< p_T >$  values were obtained by fitting  $\frac{d^2 N}{dy dp_T} \propto \frac{p_T}{[1 + (p_T / p_0)^2]^n}$  in three

different centrality bins. Low- $p_T$  excess in the most peripheral bin due to non-hadronic production.



ALICE: clear decrease of  $< p_T >$  with increasing  $N_{part}$ .

This confirms the observation that low- $p_T$   $J/\psi$  are less suppressed in central collisions.

Striking difference with respect to lower energy results!

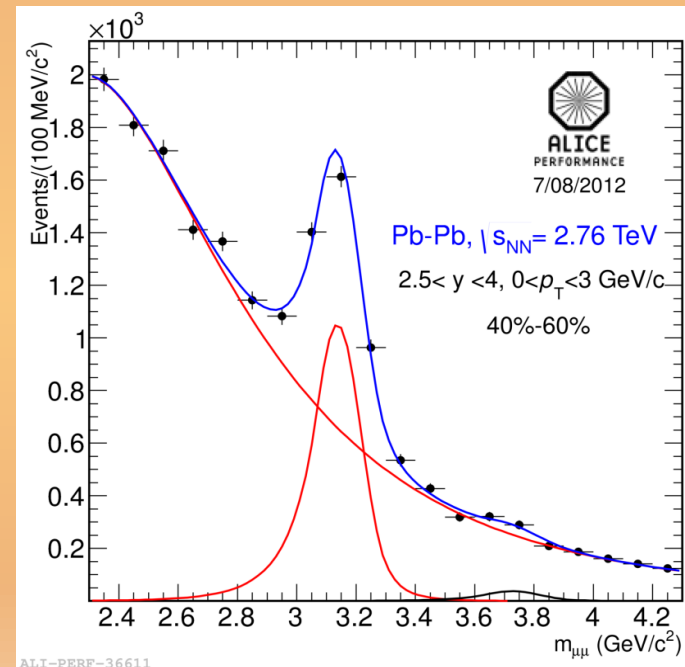
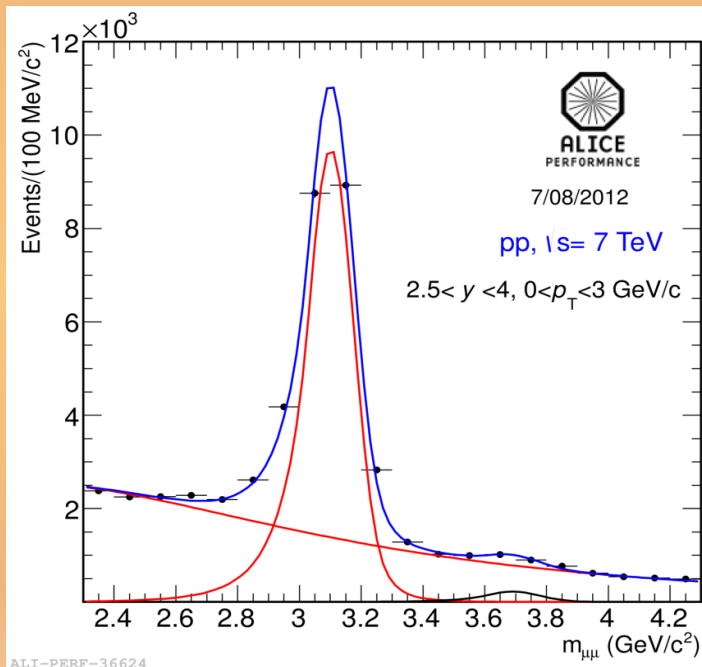
# $\psi(2S) \rightarrow \mu\mu$

Low significance for  $\psi(2S)$ , both in pp and Pb-Pb.

Signal extraction only possible in 2  $p_T$  bins:

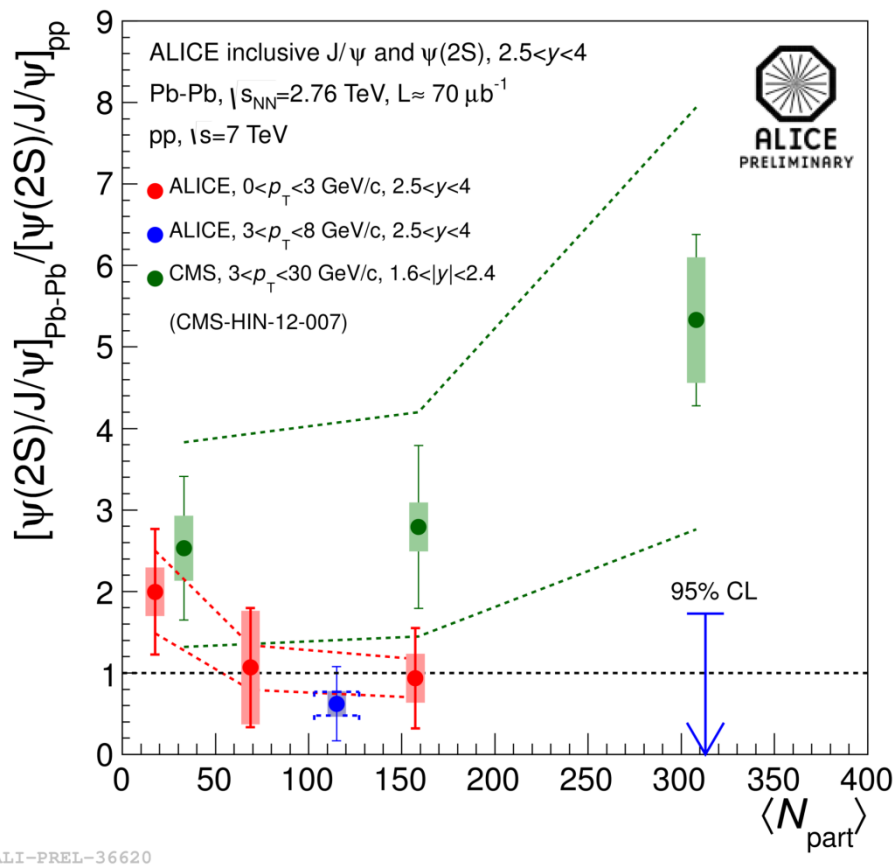
- $0 < p_T < 3$  GeV/c: 20-40%, 40-60% and 60-90%.
- $3 < p_T < 8$  GeV/c: 0-20% and 20-60%.

S/B in Pb-Pb: between 0.01 and 0.3 from 20-40% to 60-90% centrality.



# $\psi(2S) \rightarrow \mu\mu$

ALICE used pp at  $\sqrt{s} = 7$  TeV as reference: small  $\sqrt{s}$  and  $y$  dependence from  $[\psi(2S) / J/\psi]_{pp}$  results by CDF, LHCb and CMS taken into account in the systematic uncertainty ( $\sim 15\%$ ).



Dashed lines show the error on the pp reference: CMS used pp at  $\sqrt{s} = 2.76$  TeV.

Signal extraction and MC inputs for Acceptance  $\times$  Efficiency corrections are the main source of systematics (some others vanish in the double ratio).

No decisive conclusion on the  $\psi(2S)$  enhancement/suppression vs  $N_{\text{part}}$  due to large statistical and systematic uncertainties.

Excluded large enhancement in the most central collisions.

# Conclusions

- ❑ ALICE results vs  $N_{\text{part}}$  show a different behavior relative to RHIC energies:
  - Flat centrality dependence in all rapidities ( $N_{\text{part}} > 100$  at forward  $y$ ).
  - $R_{\text{AA}}^{\text{ALICE}} \sim 3 \times R_{\text{AA}}^{\text{PHENIX}}$  for the most central collisions.
  
- ❑ Hint of smaller suppression at mid rapidity than at forward rapidity in the most central collisions.
  
- ❑ Stronger suppression for high- $p_{\text{T}}$   $J/\psi$  relative to the low- $p_{\text{T}}$  ones.
  - ❑  $\langle p_{\text{T}} \rangle$  decreases with increasing centrality collision, opposite behavior compared to lower energy results.
  
  - ❑ Comparisons to models point to (re)generation.
  
  - ❑ Important to measure Cold Nuclear Matter effects.
  
- ❑  $\psi(2S)$ : No firm conclusion on enhancement/suppression with respect to  $J/\psi$ , but a strong enhancement in central Pb-Pb collisions seems unlikely.

**Backup**



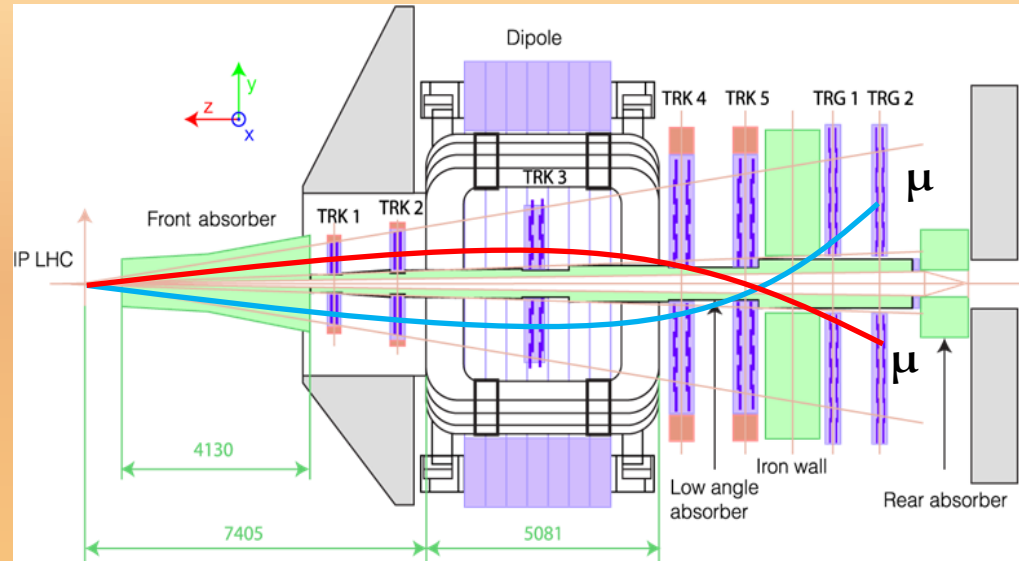
# The ALICE Muon Spectrometer

Located in the forward rapidity region and with a full azimuthal coverage, it is composed by:

- Absorbers:

- a) Front absorber.- Absorbs hadrons, photons and electrons.
- b) Beam shield.- Protects from particles produced at large  $y$ .
- c) Iron wall.- Absorbs hadrons that punch-through the frontal absorber.

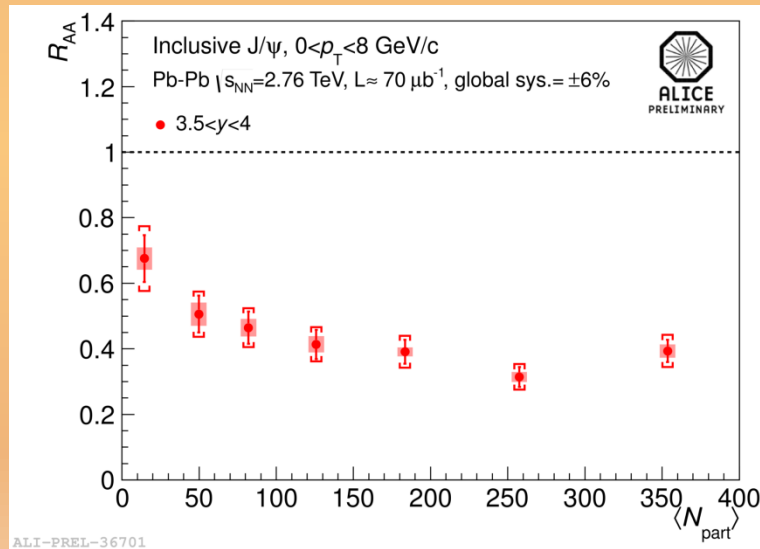
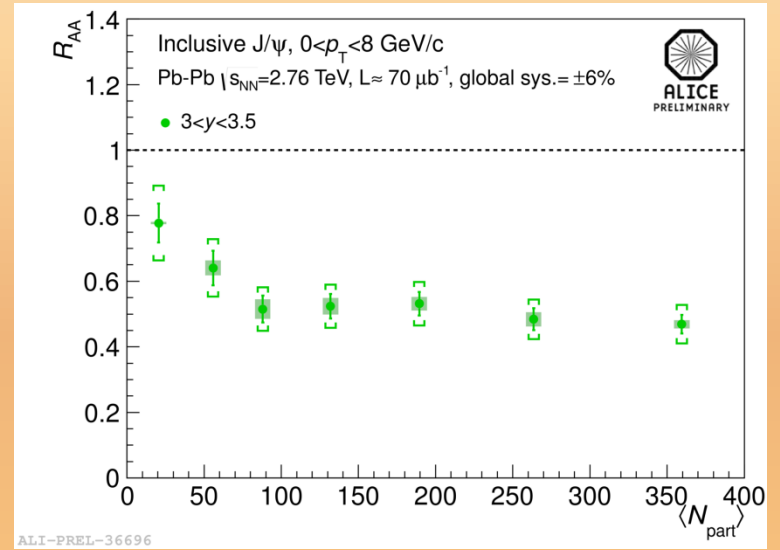
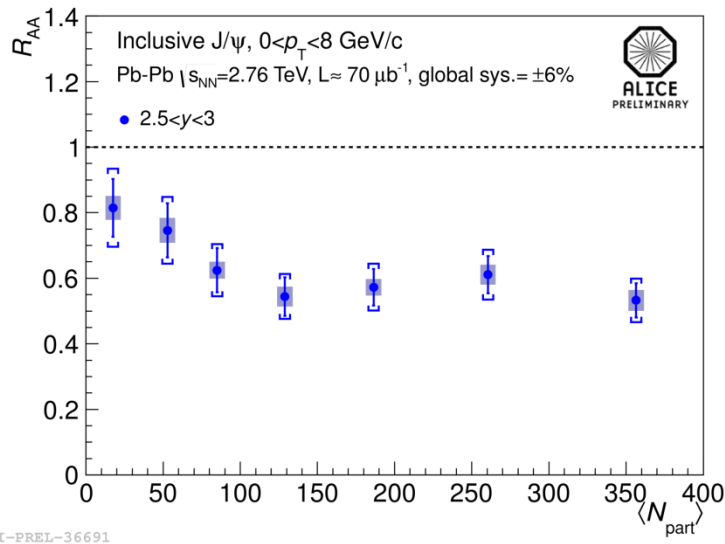
- Magnetic dipole.- 3 T·m integrated magnetic field, bends charged particles allowing to extract the sign of their electric charge and momentum.



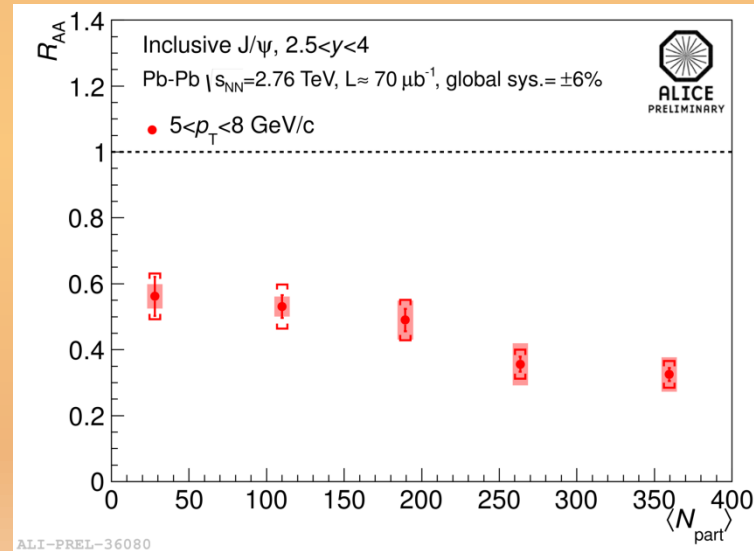
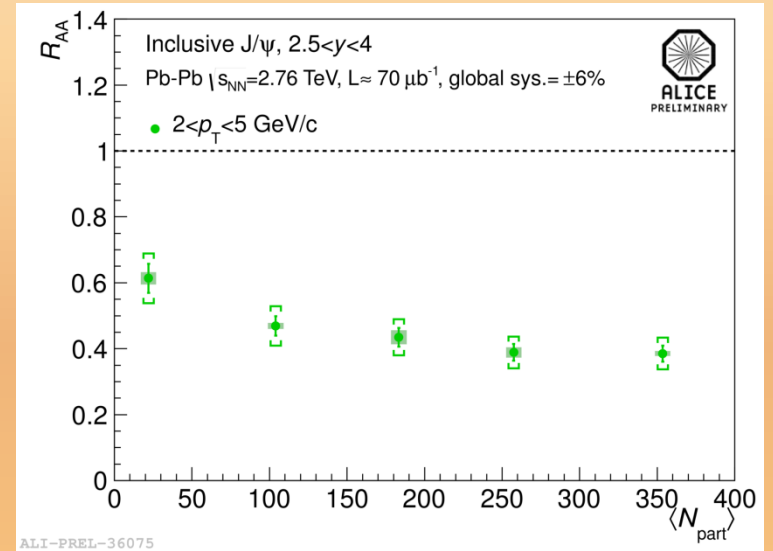
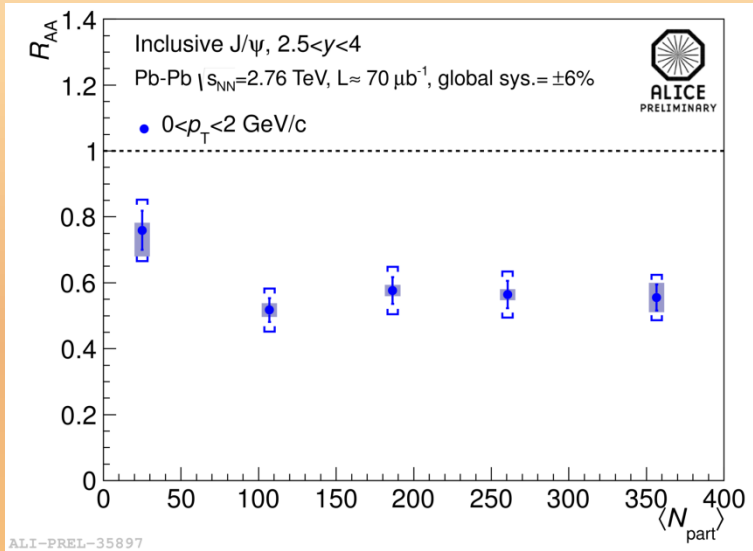
- Tracking chambers.- Spatial resolution, in bending coordinate, better than 100  $\mu\text{m}$  in order to identify and disentangle the  $\Upsilon$  family (100 MeV resolution).

- Trigger chambers.- Timing resolution of 1-2 ns and latency of 700 ns ( $L\emptyset$  trigger), can trigger likesign and unlikesign events.

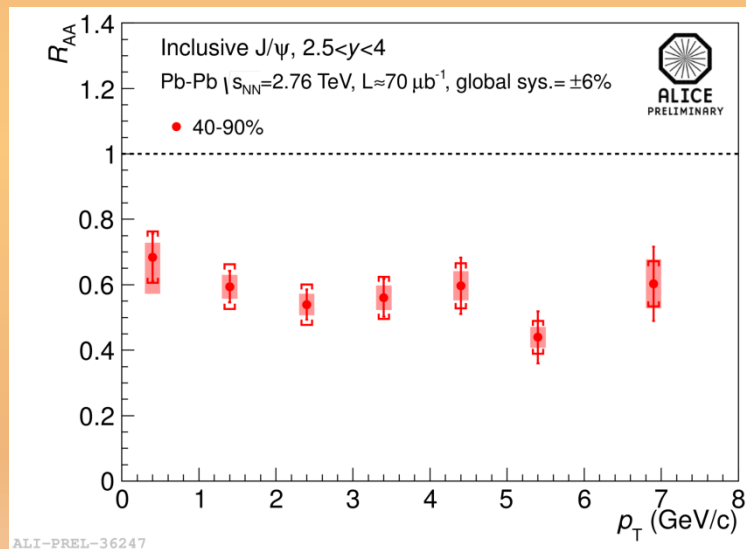
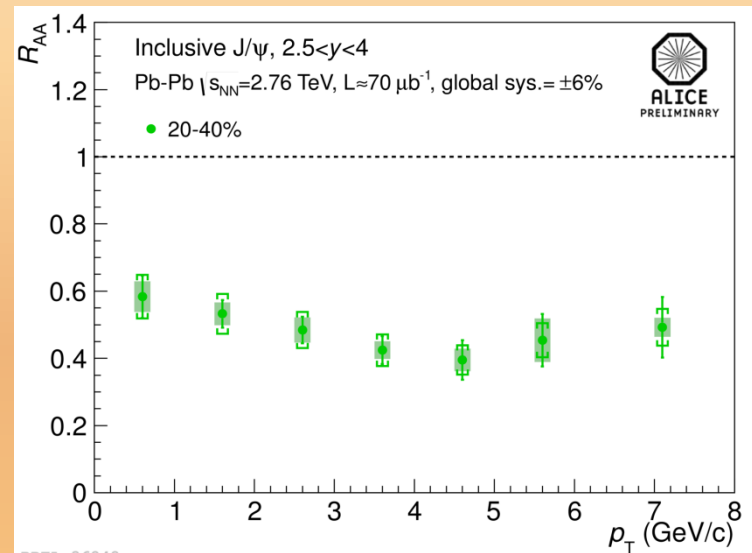
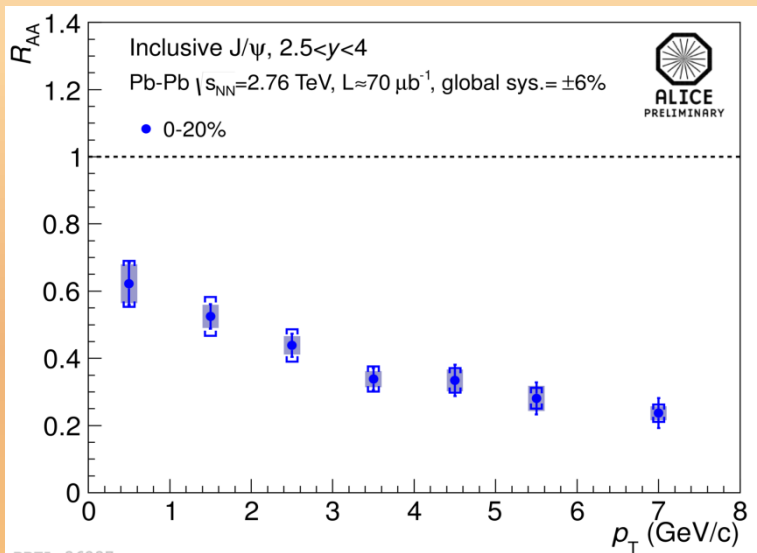
# $R_{AA}$ vs Centrality, $y$ bins



# $R_{AA}$ vs Centrality, $p_T$ bins



# $R_{AA}$ vs $p_T$ , centrality bins



ALI-PREL-36247

# Systematic uncertainties: Concepts & values

Concept	Value (%)
Luminosity pp	1.9
R factor pp	3.0
Normalization (MUL $\rightarrow$ MB)	2.1
Trigger	6.4
Tracking	6.0
Matching	2.0
MC input	5.0

# Systematic uncertainties: Integrated $R_{AA}$

Corr. systematics: MC input + Matching + Tracking + Trigger + Normalization + J/ψ pp + pp Lumi.

Unc. systematics: n J/ψ +  $T_{AA}$  + Tracking + Trigger.

Statistics: n J/ψ.

vs centrality

Corr. systematics: Normalization + pp Lumi +  $T_{AA}$  + corr. J/ψ pp.

Unc. Systematics: n J/ψ + nMB + Tracking + Trigger + MC input + Matching + non corr. J/ψ pp.

Statistics: n J/ψ + J/ψ pp .

vs  $p_T/y$

In the plots:

Statistics: vertical line at each point.

Unc. systematics: shaded area at each point.

Corr. Systematics: written at the top.



# Systematic uncertainties: Multidimensional $R_{AA}$

Unc. systematics:  $n J/\psi$ .

P.C. systematics: MC input + Matching + Tracking + Trigger + TAA + unc.  $J/\psi$  pp.

} vs centrality

Unc. systematics:  $n J/\psi$  + unc.  $J/\psi$  pp.

P.C. systematics: MC input + Matching + Tracking + Trigger + TAA.

} vs  $p_T$

Corr. systematics: Normalization + corr.  $J/\psi$  pp.

Statistics:  $n J/\psi$  +  $J/\psi$  pp .

} vs centrality/  $p_T$

In the plots:

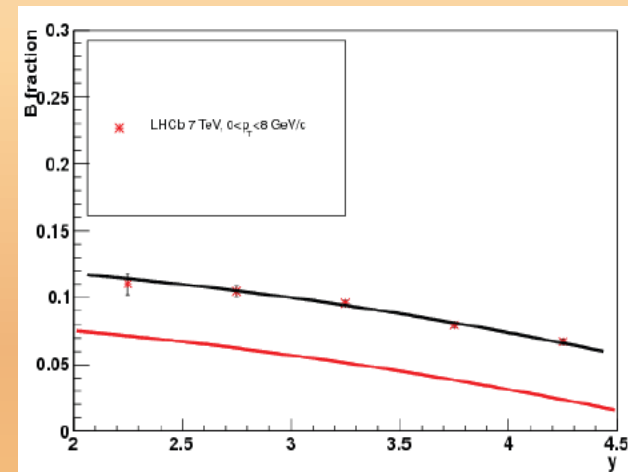
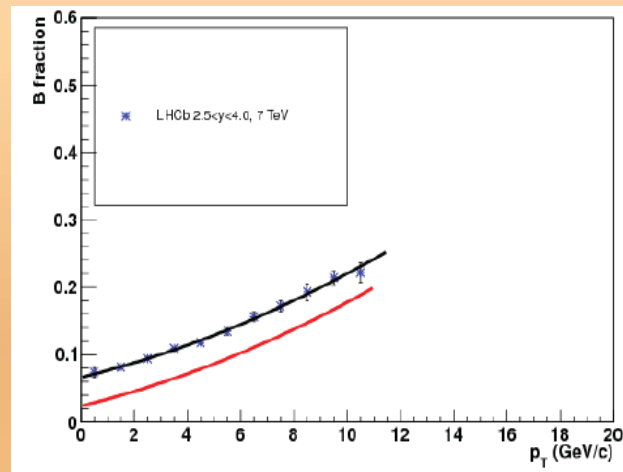
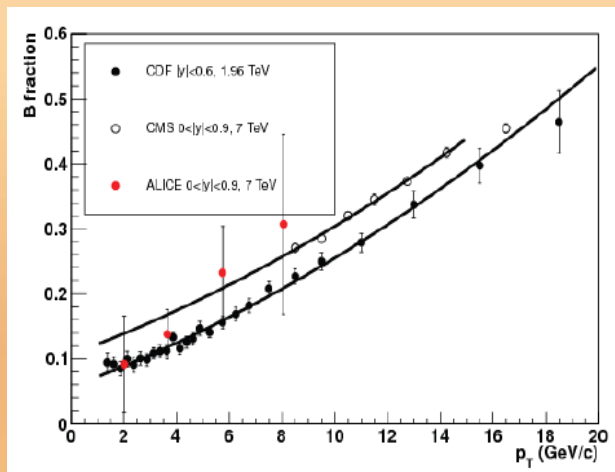
Statistics: vertical line.

Unc. systematics: shaded area at each point.

P.C. systematics: boxes at each point,

Corr. Systematics: written at the top.

# Effect of non-prompt J/ψ on ALICE $R_{AA}$



Non-prompt fraction of the inclusive J/ψ yield in pp at mid rapidity ( $f_B$ ):  
CDF vs CMS: increase of 5% and  $p_T$  independent.

Assume:

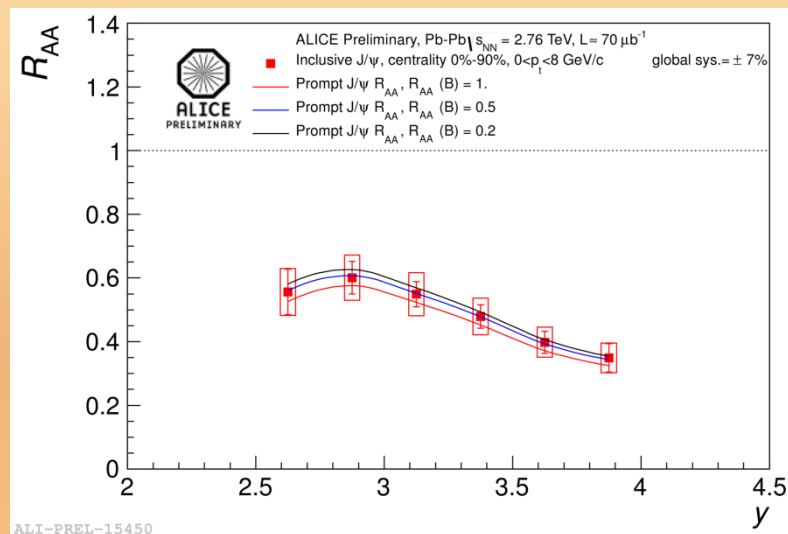
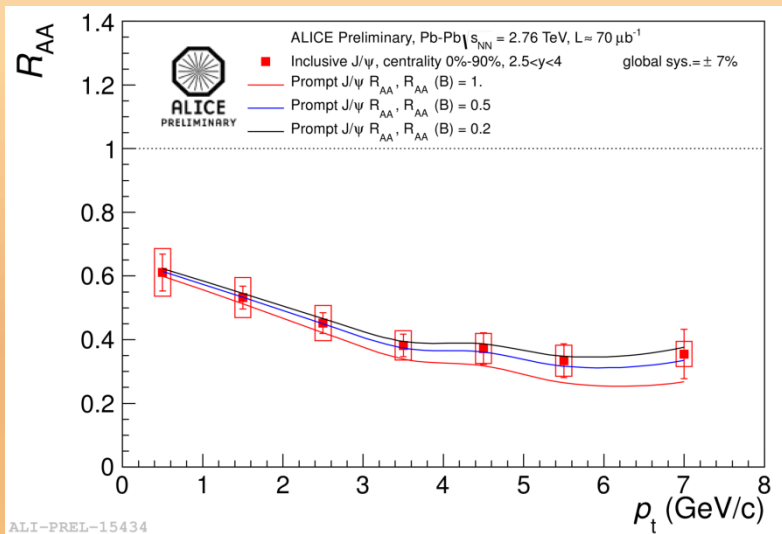
1. Linear increase of  $f_B(\sqrt{s})$ .
2. It does not depend on the  $y$  region.

}  $f_B(p_T)$  for  $\sqrt{s} = 2.76$  TeV

$b$ -hadron suppression factor in Pb-Pb ( $q$ )?  $R_{AA}^D \approx 0.3$  for  $2 < p_T < 16$  GeV/c (JHEP09 (2012) 112)  $\rightarrow$  'Dead cone effect':  $R_{AA}^B > R_{AA}^D$ .

$0.2 < q < 1$  is used

# Effect of non-prompt J/ψ on ALICE $R_{AA}$



$$R_{AA}^{\text{prompt}}(p_T) = \frac{R_{AA}^{\text{incl}} - f_B q}{1 - f_B} \quad \rightarrow \text{small effect on the inclusive J/}\psi R_{AA} \text{ results.}$$

Similar study can be carried out for  $R_{AA}$  vs  $y$ : LHCb shows  $f_B(y)$  decreases with increasing rapidity.

$\rightarrow$  Difference between inclusive and prompt  $R_{AA}$  well within errors.

# Theoretical models: inputs

## Statistical hadronization

Thermal model with  $T=164$  MeV,  $\mu = 1$  MeV (from particle ratio fits).

All charm produced in the initial hard-scatterings.

Charmonium production at phase boundary.

## Transport Model by Rapp & Zhao

Boltzman transport equation for the  $J/\psi$ .

$V_{\text{FB}}$  adjusted to measured  $dN_{\text{ch}}/d\eta$ .

$\sigma_{c\bar{c}}|_{y=3.25} \approx 0.5$  mb.

Shadowing: 30% suppression in the most central collisions.

No Croning effect and  $\sigma_{\text{Abs}} = 0$ .

10% of  $J/\psi \leftarrow B$  and no quenching.

## Transport Model by Liu *et al.*

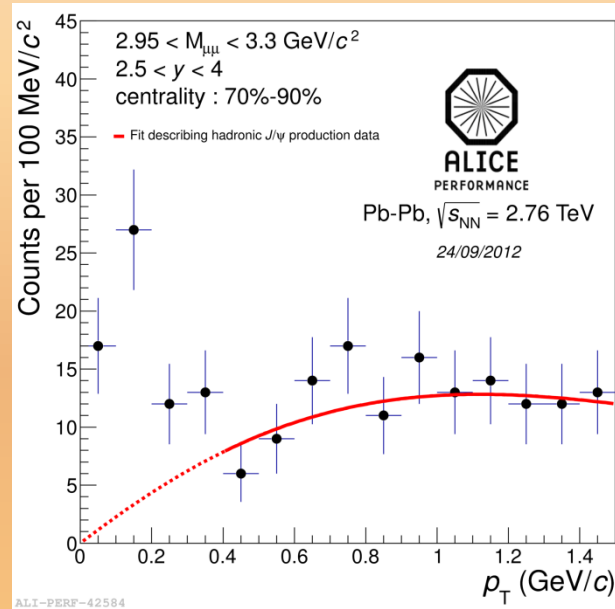
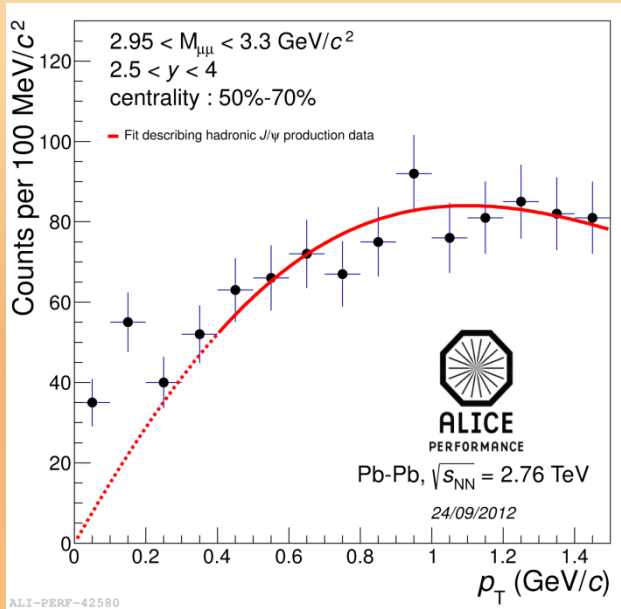
Boltzman transport equation for the  $J/\psi$ .

$\sigma_{c\bar{c}}|_{y=3.25} \approx 0.38$  mb.

EKS98 shadowing and  $\sigma_{\text{Abs}} = 0$ .

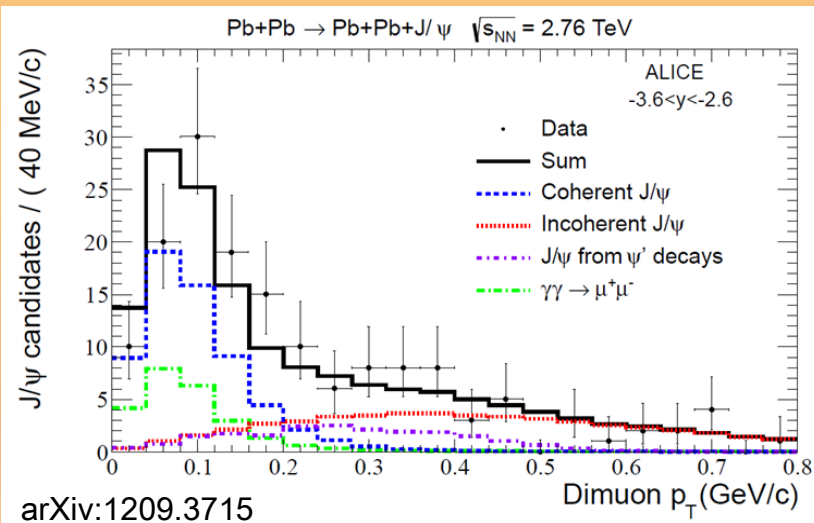
10% of  $J/\psi \leftarrow B$  and  $R_{\text{AA}}(b) = 0.4$  for all  $p_{\text{T}}$  range.

# J/ψ photo-production



Clear deviation, at low- $p_T$  for semi and peripheral collisions, to the expected J/ψ hadro-production.

J/ψ photo-production could be responsible of this excess.



More than 50% of the J/ψ from photo-production have a  $p_T$  in the 0-200 MeV/c range.

Only  $\sim 1\%$  of the J/ψ from hadro-production have a  $p_T < 200$  MeV.

arXiv:1209.3715

$$J/\psi \langle p_T^2 \rangle$$

